

Infectious diseases, imposing density-dependent mortality on MHC/HLA variation, can account for balancing selection and MHC/HLA polymorphism

D. P. L. GREEN

31 DECEMBER 2024

The human MHC transplantation loci (HLA-A, -B, -C, -DPB1, -DQB1, -DRB1) are the most polymorphic in the human genome. It is generally accepted this polymorphism reflects a rôle in presenting pathogen-derived peptide to the adaptive immune system. Proposed mechanisms for the polymorphism such as negative frequency-dependent selection (NFDS) and heterozygote advantage (HA) currently focus on HLA alleles, not haplotypes. Here, we propose a model for the polymorphism in which infectious diseases impose independent density-dependent regulation on HLA haplotypes. More specifically, a complex pathogen environment drives extensive host polymorphism through a guild of HLA haplotypes that are specialised and show incomplete peptide recognition. Separation of haplotype guilds is maintained by limiting similarity. The outcome is a wide and stable range of haplotype densities at steady-state in which effective Fisher fitnesses are zero. Densities, and therefore frequencies, emerge theoretically as alternative measures of fitness. A catalogue of ranked frequencies is therefore one of ranked fitnesses. The model is supported by data from a range of sources including a Caucasian HLA data set compiled by the US National Marrow Donor Program (NMDP). These provide evidence of positive selection on the top 350-2000 5-locus HLA haplotypes taken from an overall NMDP sample set of $\sim 10^5$. High-fitness haplotypes drive the selection of ≈ 137 high-frequency HLA alleles spread across the 5 HLA loci under consideration. These alleles demonstrate positive epistasis and pleiotropy in the formation of haplotypes. Allelic pleiotropy creates a network of highly inter-related HLA haplotypes that account for 97% of the census sample. We suggest this network has properties of a quasi-species and is itself under selection. We also suggest this is the origin of balancing selection in the HLA system.

1 Introduction

The MHC/HLA *super*-locus is a genomic region of about 150-200 loci on the short arm of chromosome 6. It covers approximately 3Mb and includes the six classical transplantation loci: class I (HLA-A, -B, and -C) and class II (HLA-DP, -DQ, -DR) [1].

HLA molecules are cell surface proteins that are germline encoded and remain unchanged for the lifetime of the holder. They act with other cellular components constantly to monitor endogenous and exogenous proteins of the internal environment of the body. Peptides derived from these proteins are mounted in peptide-HLA complexes that are presented to T-cells. T-cells recognising endogenous peptides are removed during foetal development, when foreign proteins are absent. This step limits the T-cell repertoire *post-partum* to a subset that recognizes only foreign peptides bound to HLA molecules, thereby detecting pathogen invasion.

The structural feature of HLA molecules that underpins their function is a pocket of approximately 60 amino-acids derived from exons 2 and 3 for class I alleles, and exon 2 for class II. These define a peptide-binding site (PBS). HLA class I and II loci show extensive polymorphism in these pockets. HLA class I and II loci also form numerous haplotypes that display variation through allelic permutation.

The scale of the polymorphism is large. An analysis of Caucasian five-locus HLA haplotype frequencies held by the US National Donor Marrow Program (NMDP) Registry indicates 85,000 haplotypes in a population of ≈ 6.7 million individuals [2]. Haplotype frequencies range over nearly six orders of magnitude even in this limited sample. Allele and haplotype discovery is far from complete. A cardinal feature of the HLA transplantation is balancing selection, the apparently stable existence of haplotypes and alleles at intermediate frequencies. A scan of the human genome for other regions under balancing selection found no other region, other than the ABO system, that could not be explained by neutrality [3] (although see [4] for a more recent assessment).

Observations requiring explanation include:

- allele and haplotype frequency distributions are characterised by heavy tails [2]
- linkage disequilibrium is positive ($D'_{ij} > 0$) in high-frequency haplotypes and negative ($D'_{ij} < 0$) among rare haplotypes [5]
- the Ewens-Watterson test for homozygosity shows excess homozygosity for common 5-locus haplotypes [5]
- the distribution of allelic frequencies does not conform to neutral expectations [6]
- the rate of non-synonymous nucleotide substitution significantly exceeds the rate of synonymous substitution ($d_N/d_s > 1$) in codons in the peptide-binding-region (PBR) [6]
- maintenance of alleles over long periods of time (Neanderthal/Denisovan ancestry in HLA class I alleles that has survived since the last introgression (approximately 45-50,000 years ago) [7, 8] and trans-species polymorphism in HLA class II loci that has survived since the last common ancestor (6-8 mya) [9, 10, 11])

- homogenization of introns relative to exons over evolutionary time [6]
- HLA class I supertypes [12, 13]
- frozen HLA haplotype blocks [14]
- recent selection on MHC standing variation as shown by inheritance by descent (IBD) [15, 11]
- high values of the f_{adj}^*HLA metric [16]

A list of some of the explanations for HLA polymorphism proposed over the past 50 years or so includes negative frequency-dependent selection (NFDS), heterozygote advantage (HA), overdominance, rare allele advantage, divergent allele advantage, pleiotropy, and segregation distortion balanced by negative selection. Some of these proposed explanations overlap with others or are broadly synonymous. There is no consensus theory of HLA polymorphism but the explanations of longest standing are NFDS, HA, and environmental changes over time and/or space [17], and Box 3 in [18].

There is an alternative and unexplored explanation for HLA polymorphism that rests on density-dependent regulation of individual species of HLA haplotypes by diseases.

The background to the idea is the stable existence of species diversity among Linnean species under the actions of natural selection/competitive exclusion on the one hand and limiting similarity/character displacement on the other. The theoretical basis for haplotype diversity at steady-state can be covered by the Lotka-Volterra competition equations, and density-dependent regulation by disease has its origins in the Verhulst logistic equations and the equations for disease transmission of Anderson and May [19].

This paper is divided into four sections: (i) this Introduction; (ii) an outline of relevant theoretical considerations; (iii) an analysis of the Caucasian HLA haplotype dataset available from the US National Marrow Donor Program (NMDP) together with some running commentary; (iv) a discussion of the principal findings.

2 Theoretical considerations

2.1 Background

The broad aim of this paper is to explain the frequency distributions shown by HLA alleles and haplotypes in the US NMDP Caucasian datasets. The Caucasian dataset is now sufficiently large to reveal differences in linkage disequilibrium between high- and low-frequency haplotypes and excess homozygosity for common 5-locus haplotypes [5].

Our approach is built on the assumption that HLA polymorphism is an evolved response to the pathogen environment. We are then faced with a choice: whether to incorporate population biology and proceed with density-dependence as a key element, or whether to ignore population biology and proceed with genetic explanations that are inherently limited to frequencies.

A recent review of an extensive literature on co-evolution of hosts and parasites indicates slightly less than half the papers reviewed incorporate population biology [20]. The majority that focus on frequency then split into those that follow changes in allelic or haplotypic frequencies over time, and those that invoke negative frequency-dependent selection to generate polymorphic populations through production of genotypes of approximately equal fitness. Density-dependent models can always generate frequencies by normalisation, but the reverse is not the case. Moreover, frequency-dependent models make it impossible to describe a class of non-competitive models of species coexistence in which haplotype populations are regulated independently. The most compelling reason for including population biology is the evidence that disease transmission is density-dependent.

The theoretical approaches used in this paper therefore retain density-dependence as a key foundation. Other theoretical concepts are drawn from the literature as the need arises. We start with a brief outline of a three trophic-level Lotka-Volterra model [21, 22] and the changes that need to be made to adapt it to coexistence of different genotypes of the same Linnean species. We examine the Anderson and May equations for generalised disease transmission [19] since these provide a mathematical approach to top-down forcing. A key property of these equations is the steady-state of the host that emerges under certain conditions. Steady-states can be approximated by logistic functions whose origins in the work of Verhulst [23, 24] are also examined. Finally, we introduce an important theoretical paper by Neher and Shraiman [25] that underpins our approach to the origins of linkage disequilibrium and positive epistasis in HLA haplotypes.

2.2 The three trophic-level Lotka-Volterra model of Chesson and Kuang [21]

This is outlined in Box 1 of [22]. In brief, there are three trophic levels. The focal species, in our case HLA haplotypes, occupy the middle trophic layer. The resources consumed by human hosts occupy the lower trophic level and pathogens, behaving as predators, occupy the upper trophic layer. At this point, we can start making some simplifying assumptions.

First, we remove the lower trophic level. This can be justified on a number of grounds. There is an arguable case that historically it is disease that has regulated human populations for most of human history and the prior history of primate evolution [26]. Disease has been particularly devastating in generating child mortality, driven, in part, by the immunological naïvety of children. Second, we are seeking an explanation for a major evolutionary adaptation, the HLA system, that appears unequivocally to be related to defence against disease and little else. That indicates selective pressure exercised by diseases over an extended time frame. This is not to dismiss the importance of famine and starvation as immanent parts of existence, and there is no doubt about the potentiating interaction of malnutrition and disease. This could, in principle, lead to resource-based input into competition between HLA haplotypes. However, to be set against that is the rapid population expansions following improvements in public sanitation and supplies of potable water in the latter part of the 19th century, followed by widespread vaccination in the 20th. These changes produced major reductions in child mortality.

A second change is not to pursue the resource consumption rates. These serve little purpose

once the lower trophic level is removed. Moreover, the pathogen environment of the upper trophic layer is not a typical predator, and we have no easy way of calculating its energy extraction from the focal species.

Armed with these changes, we end up with a simple system where pathogens exercise downward pressure on a focal species related to its density, thereby counterbalancing its incipient tendency to grow. We go one further, however, by dividing the focal population into a guild of molecular species, where a guild has the sense used in ecology; a group of species that exploit the same class of environmental resources in the same way. The species are molecular variants of a single Linnean species.

The molecular guild under scrutiny in the current case is the HLA system of peptide presentation. We propose the effect of the pathogen environment, as sensed by the HLA system, is to reduce the individual densities of the major HLA haplotypes and spread their number. Limiting similarity between haplotypes establishes a set of silos. Variation within silos is then restricted or eliminated by competitive exclusion. Major haplotypes within silos move to zero fitness at steady-state. Effective fitness differences therefore disappear and silos show stable coexistence.

2.3 Density-dependent regulation of population by disease

Early mathematical models of disease transmission used populations of fixed size and studied changes in the frequency of different disease states in the host. Many had their origins in the work of Ronald Ross on malaria and the compartmental model of Kermack and McKendrick [27, 28, 29]. The Kermack-McKendrick model identified three states (Susceptible, Infectious, Recovered/Removed) and introduced equations to account for changes in frequency of the three states.

The first work to treat densities of S, I, and R populations as dynamic variables was that of Anderson and May [30, 19]. Their model took the three standard SIR states (Susceptible, Infectious, Recovered) and assigned them densities X , Y , and Z , respectively. It proceeded with rate equations that are, effectively, mass action equations [19]. The important figure in [19] is Fig.3, where the infection step is shown as the equivalent of bi-molecular collision between infected carriers and susceptible individuals. Equation (14) in their paper [19] shows a second-order rate constant β in the denominator. This step creates the density-dependence of infection, since all other rate constants are first order.

Fig.1 in the current paper is a redrawn version of Fig. 4a in [19]. Anderson and May treat the population in their Fig. 4a as genetically homogeneous. Curve (a) in Fig.1 of the current paper represents population growth in the absence of disease; curves (b), (c), (d), and (e) represent changes in population density in endemic disease where precise behaviour rests on the duration of immunity. Our Fig.1 shows that host populations will be capped under certain conditions and is the basis for population regulation of the host or focal species. If there is no immunity, individuals are maximally susceptible, and the population may fail to expand above the threshold, as shown by line (e) to the right of the arrow head. The threshold population density, N_T , has its origin in the Kermack-McKendrick epidemic threshold [31] and is the population density below which infection dies out. The existence of an epidemic threshold is potentially of fundamental importance in protecting low-density populations from extinction by disease and drift.

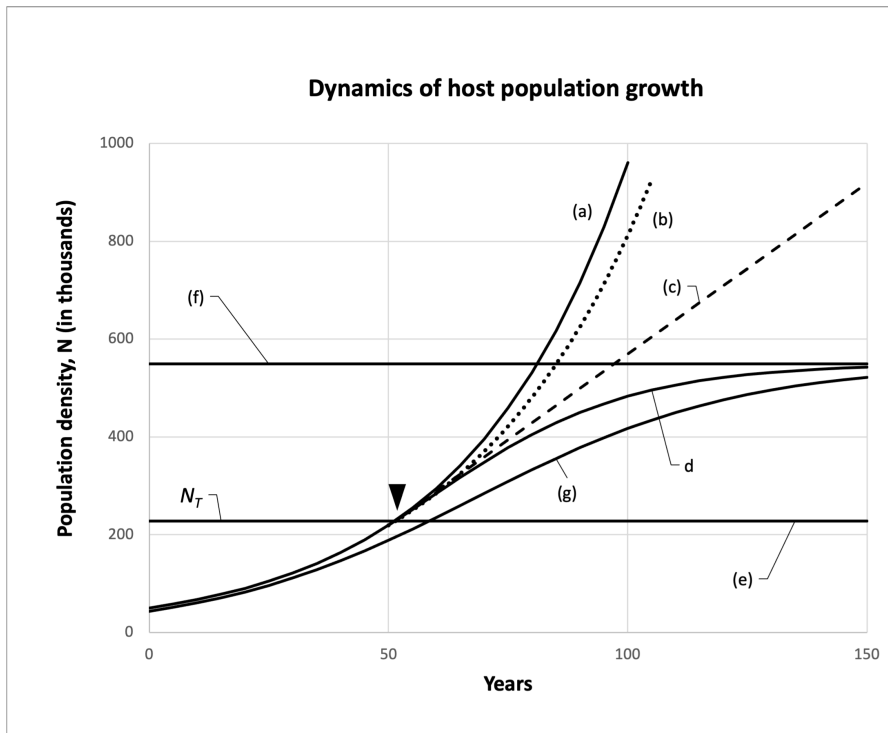


Figure 1: Adapted from a similar figure in [19]. The timeline in Years and Population density are both imported from the original. Line (g) is a plot of the logistic equation whose asymptote, N^* , is the same as for (d). The arrow head indicates the time point at which the population density exceeds the threshold for disease transmission effects to emerge.

Our Fig.1 also contains a logistic equation plot (g) whose asymptote, N^* , is the same as a population brought to steady-state by disease (Eq.14 in [19]). This has a direct bearing on the model outlined in the next subsection (2.4) since, as in the previous subsection (2.2), the population is divided into distinct molecular species. It is assumed the Anderson-May model can be applied independently to each major HLA genotype population. This assumption is underpinned by a direct connection to the extensive review by Anderson and May [32] in which the idea is put forward that polymorphism of host defence alleles can be modeled by density-dependent logistic functions. This, in turn, has direct relevance to the stability of co-existing populations at steady-state [33].

2.4 The Verhulst logistic equation and Loka-Volterra competition equations

The idea that populations expand geometrically and indefinitely can be traced back to Euler [34, 35, 36]. Malthus was apparently the first to be interested in limitations to geometric growth imposed by limited resources, and his Essay on the subject [37] was widely influential. It had a major impact on Darwin, who read the Essay in 1838. Verhulst also read the Essay and published a general equation for capped population growth

$$\frac{dN}{dt} = rN - \varphi(N) \quad (1)$$

where r is the net growth (birth *minus* death) rate constant, N is the population density, and $\varphi(N)$ is an additional mortality rate that is some function of N [23, 24]. (Verhulst's symbols have been changed from those in his paper to their common modern usage.) Verhulst chose $\varphi(N) = \alpha N^2$ from a number of possibilities, since it best fitted the census data on the rate of growth of populations in the first decades of the 19th century, of which the French census data were the most important because of their size and thoroughness. The Verhulst equation is, therefore,

$$\frac{dN}{dt} = rN - \alpha N^2 \quad (2)$$

or, expressed as the per capita change, is

$$\frac{1}{N} \cdot \frac{dN}{dt} = r - \alpha N \quad (3)$$

where r is Fisher's intrinsic fitness. The integrated form of Eq. 2 is Verhulst's logistic equation.

Verhulst's work fell into desuetude in the latter part of the 19th century. His logistic equation was developed independently by McKendrick and Kesava Pai [38], and rediscovered by Pearl and Reed in 1920 [39]. Pearl and Reed gave it the widely-used form

$$\frac{dN}{dt} = mN = r \left(1 - \frac{N}{K}\right) N \quad (4)$$

where

$$\frac{1}{N} \cdot \frac{dN}{dt} = m = r \left(1 - \frac{N}{K} \right) \quad (5)$$

m is the effective fitness and Fisher's Malthusian parameter. Verhulst obviously knew that the value of K would be the upper limit for the population density when $t \rightarrow \infty$ and $dN/dt = 0$ since he called it '*la limite supérieure de la population*' [23]. It subsequently came to be regarded as a carrying capacity, acquiring the widespread status of an independent variable. In reality, it is set by the balance between r and α , since $r/\alpha = K$ at steady-state. Mallet has written an extensive review of $r - \alpha$ and $r - K$ formulations, arguing, correctly in our view, for the merits of the $r - \alpha$ form [40].

This is an important distinction in the context of our paper since the resource layer has been set aside as a source of population regulation. We have argued instead that, to a first approximation, we are dealing with a contest between expansion of a focal host population of haplotypes and an upper trophic layer that responds negatively to emerging haplotype densities in the host guild.

2.5 Fitness and natural selection in a population at steady-state

Steady states in the current context exist when $dN/dt = m = 0$. At steady state, $r = \alpha N^*$, where N^* is the steady-state density (N^* being the formulation used in [19]). Since r is a measure of fitness, so must αN^* be. The values of α and r cannot be measured directly, but the values of N^* emerge as relative abundances or frequencies. For molecular species within a single Linnean species, one can make the assumption that r , or at least the average, \tilde{r} , is the same for each genotype.

If $\tilde{r}_i = \alpha_i N_i^*$ for the i th population at steady-state, and $\tilde{r}_1 = \tilde{r}_2 = \dots = \tilde{r}_i = \dots = \tilde{r}_n$, then $\alpha_i N_i^*$ is the same for each genotype and

$$\alpha_1 N_1^* = \alpha_2 N_2^* = \dots = \alpha_i N_i^* \dots = \alpha_n N_n^* \quad (6)$$

However, the values of α_i and N_i^* need not be the same, since only their product is equal to \tilde{r} . Instead, their values pivot; the larger the value of N^* , the smaller the value of α , and vice-versa.

A simple example will illustrate how useful this can be in the case of infectious disease. We take an immunologically naïve population and immunise a proportion against a disease such as smallpox. We assume the immunisation itself is harmless and produces no morbidity or mortality. The total population is then exposed to smallpox. The immunised population shows a fitness represented by curves (a) or (b) in Fig. 1. By contrast, the unimmunised population is capped at a much lower density. If we assume both populations reach steady-state, the density of the immunised population is much higher than that of the unimmunised population. Its value of N^* is higher, and its α is smaller although the *per capita* rates of growth are zero in both cases. We regard the immunised steady-state population as fitter because it has a higher density and higher frequency. A rank order of genotypic frequencies is a rank order of fitnesses, and the two can be plotted against each other, as in Figs. 2-7 below.

One can also re-write Eq. 6 as a special case where the logistic equation is applied to the full range of population expansion:

$$\frac{m}{r} + \frac{N}{N^*} = 1 \quad (7)$$

Stated verbally, the ratio of the Malthusian parameter to Fisher's fitness, plus the ratio of actual population density to the ultimate steady-state value, is equal to unity. This equation demonstrates a conservation of fitness.

This is also a convenient opportunity to introduce conditions around stability of steady-states involving the co-existence of multiple species. An important, widely quoted, contribution was made by Levin [41]:

No stable equilibrium can be attained in an ecological community in which some r components are limited by less than r limiting factors. In particular, no stable equilibrium is possible if some r species are limited by less than r factors.

Like us, Levin eliminated the restriction that all species are resource limited and wrote the following in his Summary:

... if two species feed on distinct but superabundant food sources, but are limited by the same single predator, they cannot continue to coexist indefinitely. Thus these two species, although apparently filling distinct ecological niches, cannot survive together. In general, each species will increase if the predator becomes scarce, will decrease where it is abundant, and will have a characteristic threshold predator level at which it stabilizes. That species with the higher threshold level will be on the increase when the other is not, and will tend to replace the other in the community. If the two have comparable threshold values, which is certainly possible, any equilibrium reached between the two will be highly variable, and no stable equilibrium will result.

(Levin's threshold level is the steady-state.) The case of smallpox infection is of a single limiting factor. It follows that only inoculated individuals will prosper long-term and, other things being equal, immunologically-vulnerable individuals will either exist at low densities or drift to extinction.

2.6 Lotka-Volterra competition equations

The parallel use of equations such as Eq.4 led to a large literature on the co-existence, stable or otherwise, of Linnean species. The simplest case is of two capped species that live independently and make no claims on resources used by the other. This simple arrangement is likely to be rare in practice, because some competition for resources of one sort or another is almost inevitable in a resource-based model, and claims on each other are likely to arise. This is the territory of the Lotka-Volterra competition (LVC) equations where two or more species compete in the same trophic layer. The equations for the two populations are

$$\frac{dN_1}{dt} = (r_1 - \alpha_1 N_1 - \alpha_{12} N_2) N_1 \quad (8)$$

and

$$\frac{dN_2}{dt} = (r_2 - \alpha_{22}N_2 - \alpha_{21}N_1)N_2 \quad (9)$$

where the third term in the bracket of Eq.8 represents the claims by population {2} on the resources that would otherwise be available entirely to population {1}, and Eq.9 represents the reverse case. When $dN_1/dt = dN_2/dt = 0$, one solution is that $(r_1 - \alpha_{11}N_1 - \alpha_{12}N_2)$ and $(r_2 - \alpha_{22}N_2 - \alpha_{21}N_1)$ are both equal to zero. The equations can be drawn graphically, with linear isoclines, $(r_1 - \alpha_{11}N_1 - \alpha_{12}N_2) = 0$ and $(r_2 - \alpha_{22}N_2 - \alpha_{21}N_1) = 0$. Stable co-existence occurs if $r_1/\alpha_{12} > r_2/\alpha_{22}$ for $N_1 = 0$ and $r_2/\alpha_{21} > r_1/\alpha_{11}$ for $N_2 = 0$. Put verbally, the two species may coexist at some steady-state or equilibrium, or one may always exclude the other. It is sometimes said that one species can win depending on initial conditions, implying that a win is not always inevitable if initial conditions are different. The simple co-existence case arises if α_{12} and α_{21} both equal zero.

The use of LVC equations has been extended to much larger numbers of distinct populations. More generalised forms of the equations were introduced some 40 years ago [42, 43] for a community of Linnean species that take the general form

$$\frac{dN_i}{dt} = N_i \left(r_i - \alpha_i N_i - f \left(\sum_{j=1}^S \alpha_{ij} N_j \right) \right), j \neq i \quad (10)$$

where i runs over a pool of S species' populations, with N_i , r_i , and α_i as their population density, intrinsic growth rate constant (= intrinsic fitness), and self-regulation (density-dependent mortality) constant, respectively: f is the functional response, and $\alpha_{i,j}$ are the interaction coefficients of other species making claims on resources that would otherwise be available entirely to species i . Versions of Eq.10 have been used to model resource competition in ecological communities [42], community food webs [44], plant communities [45], and plant-animal mutualistic networks [46].

2.7 The Neher-Shraiman (NS) model (2009)

Interpretation of data in the current paper has been informed by a theoretical approach developed by Neher and Shraiman [25, 47]. Their paper used computer simulation to examine the balance between selection on recombination and epistasis respectively in determining the outcome for a set of polymorphic loci on a hypothetical haploid chromosome that undergoes sexual reproduction. A key finding is that "clonal condensation" occurs when the recombination rate falls enough for epistatic alleles derived from a group of loci to behave as a single *super*-allele or haplotype and undergo selection accordingly. If the positive epistatic effects are large enough, a haplotype rises to fixation through competitive exclusion and is the fittest haplotype, measured in terms of Fisher's fitness.

An important theoretical component of [25, 47] is the separation of haplotype fitness, F , into two components, epistatic, E , and additive, A , such that:

$$F = E + A \quad (11)$$

The fitness of the additive component is heritable in the sense that haplotype fitness is determined by the independent fitnesses of the contributory alleles, with no positive epistasis. If haplotypes differ in additive fitness, it is due to differences in the intrinsic fitness of the alleles. By contrast, the epistatic component reflects the ability of some allelic combinations to perform more effectively than others, with heightened fitness and selection for expansion to high frequencies. The highly-fit haplotype passes unaltered to progeny but is occasionally broken up by recombination, thereby imposing a recombinational load. Underlying the NS model is an environment where all haplotype clones that come under selection are subject to competitive exclusion and only one emerges as the fittest. Polymorphism would be inherently unstable if haplotypes had markedly different fitnesses. This outcome is obviated if the high-frequency haplotypes are independently regulated, irrespective of the source of regulation. We nominate disease because it is manifestly connected to HLA function and the theoretical epidemiological underpinning has been known and accepted for decades.

A major focus of the NS model is the ability of clonal populations with one or a few major clones to adapt in a timely way to a shifting environment that requires adoption of new mutants if population fitness is to be maintained. The possibility that HLA haplotypes are at risk of slow response to a pathogen environment that can change rapidly to avoid peptide presentation is obviously a matter of concern, not least because so much of the analysis in this paper collapses if medium- to long-term steady-states are unattainable.

A brief interpolation is given here to help interpretation of the NMDP data. Concerns, inasmuch as they affect the HLA presentation of peptide, are two-fold. First, standing variation is greatly increased if many different haplotypes are stably retained in parallel, rather than eliminated. Multiple morphs can be stabilised by the limiting similarity that follows haplotype specialisation in complex environments. The second concern is an assumption that a rapidly changing pathogen environment requires HLA haplotypes to change rapidly. We argue this assumption is fundamentally wrong. The evolved solution to the challenge of pathogen escape is the stable existence of numerous, moderately low-affinity HLA haplotypes, not rapid turnover of HLA specificities.

2.8 Belevitch

The following is a brief summary of a linguistic analysis developed by Belevitch [48]. It is included because it provides an insight into outcomes obtained from log rank-log frequency plots, which are used in this paper to analyse the frequency distributions available from the US NMDP.

Any plain language text has elements (letters, words, sentences, etc.) that can be counted. Dividing these counts (say, of specific words) by the total number of words in the text gives relative frequencies or *a priori* probabilities for each word. One can also construct catalogues for each linguistic element (dictionaries for words, for example) where each distinct element (word) is listed with its probability of occurrence in the text. These words can be ranked in order of non-increasing probabilities. Some elements (words) only occur once and these define the unit probability or frequency of occurrence for a particular text. All other elements have frequencies in the text that are whole-number multiples of the singleton frequency. Since the number of ranks is equal to the number of dictionary entries, each rank is associated with a whole-number multiple of the singleton frequency.

There are two additional properties of statistical linguistics that are absent in general statistics. One is the closure condition

$$\sum_{i=1}^{i=N} N_i p_i = 1 \quad (12)$$

The other is that, in information theory, there is an entropy, x , that is related to probability by

$$x = -\log p \quad (13)$$

The entropy x can be plotted against rank. A property of dictionaries with large numbers of low-frequency elements is that the behaviour of the bulk of the population is represented by a relatively small number of entropies in a small part of the rank order range. For that reason, it is more useful to plot log rank against entropy, which is rank *versus* probability (or frequency) on logarithmic co-ordinates.

There can be no *a priori* expectation for the shape of the resulting distribution, but the local value of the slope of a tangent at a particular point in the distribution potentially has value. Belevitch established the gradient of the log rank-log frequency distribution for an arbitrary distribution function $\varphi(x)$ in the neighbourhood of a point x_0 using a Taylor expansion and arrived at the expression

$$\log \frac{p_i}{p_0} = -A \log \frac{i}{i_0} \quad (14)$$

where an element with entropy $x = x_i$ has a probability $p_i = e^{-x_i}$ and rank i . Similar notations p_0 and i_0 apply to a nearby reference point x_0 , which may be the frequency of the highest-ranked element. Eq.14 is independent of any assumption about the distribution law, with A merely measuring the slope of the tangent at x_0 to the rank-frequency characteristic on logarithmic scales. There is an obvious connection to a community of elements, such as haplotypes, at steady-state.

2.9 Our model

Considerations covered in subsections 2.1 to 2.8 lead to a simple model, stated here for a single HLA haplotype. Haplotype {1} presents peptides from pathogen A but not B. {1} is immune to A by virtue of its successful peptide presentation and a population of {1} would expand, in the absence of B, following curve (b) in Fig.1 (this paper). In the presence of B, {1} will be regulated and follow a curve such as (d) to a density-regulated steady-state population size. At worst, B may be sufficiently pathogenic that {1} cannot grow above the Kermack-McKendrick threshold. Haplotype {1} is therefore regulated by B but safe from extinction. The same applies to haplotype {2}, which presents peptides from pathogen B but not A.

This model is scaled up to account for extensive HLA polymorphism, which can be regarded as a large-scale community of genotypes. Large-scale communities have raised issues about stability for more than 50 years [49, 50, 33]. Random matrix theory (RMT) has played an important rôle over that time (see introduction to [51] for a brief up-to-date overview). A key element in the approach to stability has been the asymptotic linear stability of an equilibrium

point. Large-scale Lotka-Volterra models of the form in Eq.10 are increasingly commonly used. For example, a recent two-trophic-level predator-prey model has 200 predators and 800 prey species [51].

We argue in the current paper that the number of HLA haplotype species under selection in the Caucasian dataset is of the order of 350-2000. Bearing in mind Levin's restrictions on the number of species that can co-exist in a stable equilibrium [41], there must be a similar or greater number of limiting factors. In this paper, the limiting factors are pathogens. A set of 350-2000 haplotypes is consistent with an estimated 1400 or so human pathogens [52], some of which will exist as multiple major strains [16, 53].

3 Results: Data analysis

3.1 Log-log rank-frequency plots: HLA 5-locus haplotypes

A distinguishing feature of HLA polymorphism is its scale. Even now, after decades of work, the rate of discovery of new HLA class I and II alleles shows no sign of saturation (see, for example, Fig.2 in [54]). The term *hyperpolymorphism* has entered the language [54]. The largest datasets that give direct access to the scale of HLA polymorphism are those assembled by the US National Marrow Donor Program (NMDP). These are accessible through <https://www.nmdp.org>. A fuller description of the development of the NMDP database is given in [55]. The NMDP files have the bottom $\sim 1\%$ of the census population removed. We also use a set of frequencies derived from the NMDP data using an expectation-maximisation (EM) algorithm [5]. This set is complete. Assuming the minimum frequency is the unit frequency, the sample has a census value of 14,947,683 haplotypes, covering 101,230 different haplotype species. There are no accompanying identifiers in the EM set. A log-log plot of the two sets against each other shows no obvious anomalies, but extends only to haplotype species of rank 37645. This accounts for 99.08% of the census population.

NMDP haplotype frequencies are listed under 13 self-identified ethnicities (Caucasian, Hispanic, American Indian, etc.). We have examined data for all 13. However, we have mostly used data for the Caucasian population, which is substantially larger than the others, particularly the five-locus Caucasian haplotype HLA-A \sim B \sim C \sim DRB1 \sim DQB1. Other similar sets of data are available from the Anthony Nolan register, but these are much smaller. For example, the British/Irish/North-West European (BINWE) set in the Nolan registry, which is likely to have a similar ethnicity to the NMDP Caucasian set, has only 4% of the NMDP coverage. The distribution of Caucasian 5-locus HLA haplotype frequencies from the NMDP set is shown in Fig.2 (red markers). It demonstrates close approximation to a power law distribution for the first 300 or so haplotypes by rank (black line). The blue line represents the expected values for the same 5-locus HLA haplotypes calculated from the equilibrium frequencies of individual contributing alleles.

The data from frequency data in Fig. 2 can be plotted on logarithmic co-ordinates (Fig. 3). Following Belevitch [48], the ordinate can also represent entropy values. The red markers represent Shannon entropies. The first ≈ 350 haplotypes ($\approx 58\%$ of the census population) lie

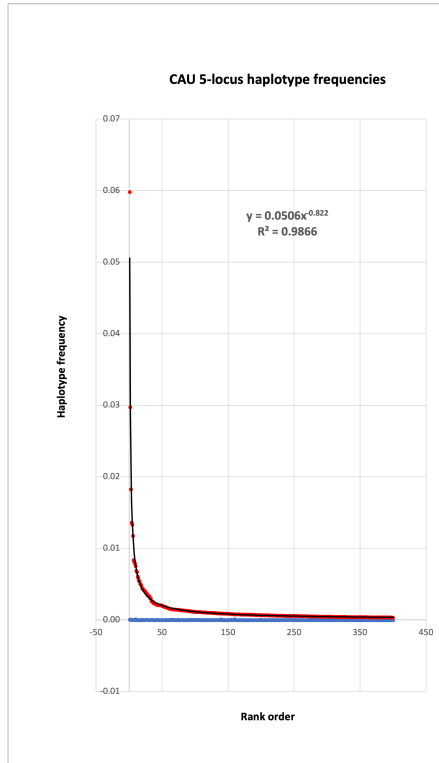


Figure 2: The US NMDP Caucasian HLA 5-locus data set plotted on linear co-ordinates for the 400 haplotypes of highest frequency. Red markers are actual frequency values. Blue markers reflect calculated haplotype frequencies based on multiplication of allele frequencies; that is, equilibrium values. The black line is the least-squares fit to the red data. The curve is closely fitted by the simple power relationship, $y = 0.0506x^{-0.822}$.

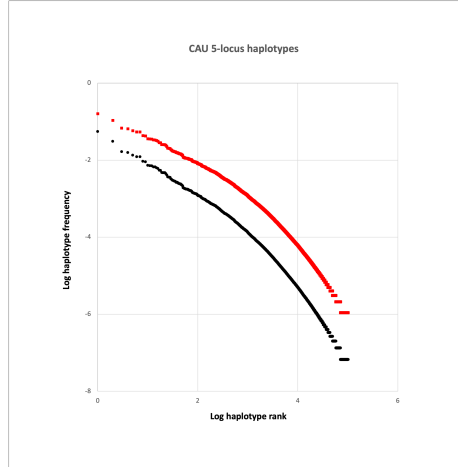
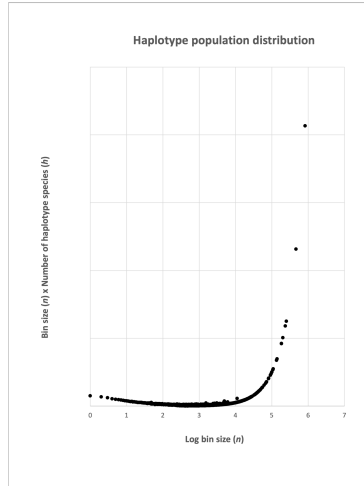


Figure 3: The NMDP Caucasian HLA 5-locus data set after use of an EM (Expectation-Maximisation) algorithm [5] (black markers). The frequencies in the linear portion are consistent with positive selection on haplotypes, with an underlying niche apportionment possibly acting on a haplotypic HLA population behaving as a quasi-species. The curved portion reflects progressive loss of positive selection and its replacement by drift and possibly negative selection, consistent with changing sign for D'_{ij} [5]. The red markers represent the distribution of Shannon entropies of individual haplotypes ($S_i = -p_i \ln p_i$) on the same axes.

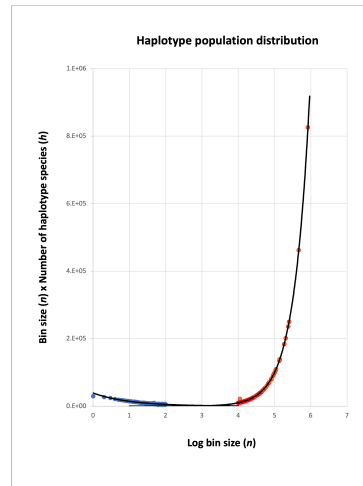
on a straight line whose gradient of -0.813 is the constant -A in Eq.14. The extensive linear portion of the distribution indicates underlying niche apportionment.

The data in [5] can be plotted in other ways. For example, each haplotype species is associated with a census frequency that indicates how many copies of that haplotype exist in the sample. These frequencies are integral multiples of the unit frequency shown by a haplotype species that occurs only once. One can construct histograms from these data in which the frequency multiples, n , including those for which there are no actual haplotypes, are listed in order on the abscissae of Figs.4a,b. The ordinate represents the number of times, h , the sample includes different haplotype species with a given frequency multiple (described as bin size, n). By way of illustration, there are $h = 30002$ haplotype species in the Alter et al. sample [5] that occur only once ($n = 1$), $h = 13604$ haplotype species occur twice ($n = 2$), $h = 8163$ three times ($n = 3$), and so on. At the upper end of the frequency spectrum, there are separate haplotype species that occur $n = 826429, 462799, 250191$ times, etc. but these frequency multiples are each associated with a single haplotype that is different in each case ($h = 1$). Most high-frequency multiples are absent. The outcome of a plot in which hn is plotted against n is highly informative (Figs.4a,b). The ordinate is linear and the abscissa is logarithmic. The sum of the hn values for all actual n is the CAU haplotype sample size (= 14,947,683).

Figs.4a,b provide clear evidence of two haplotype populations that have limited overlap.



(a) Abscissa: bin size, n , is the number of times a haplotype appears in the catalogue. Bin sizes are integers and run continuously from 1 to 10 million on logarithmic scale, irrespective of whether bins are filled or empty. Ordinate: the total number of haplotypes in a bin, $h \times n$, where h is the number of haplotypes whose catalogue frequency matches a particular bin size. The scale is linear. The plot shows two distinct populations with limited overlap. That on the left of the minimum contains haplotypes that are subject either to drift or mild negative selection. That on the right of the minimum contains haplotypes under increasing positive selection as one moves to the right.



(b) Data used in Fig.4a showing fitting of two exponential curves. That on the right is for bins in which $h = 1$, with one exception where $h = 2$. Since n is plotted against n , one on linear, the other on logarithmic co-ordinates, the curve is exponential ($y = 1.0378e^{2.2947x}$; $R^2 = 0.9999$). The best fit of an exponential for the left-side population is slightly poorer ($39074e^{-0.993x}$; $R^2 = 0.9514$), reflecting the increasing stochasticity of h values associated with small haplotype numbers in small bins. Blue markers show data used for left-side population exponential, red markers for right-side.

Figure 4: Distribution of census haplotype numbers by product of haplotype species number and bin size, $h \times n$, against bin size, n .

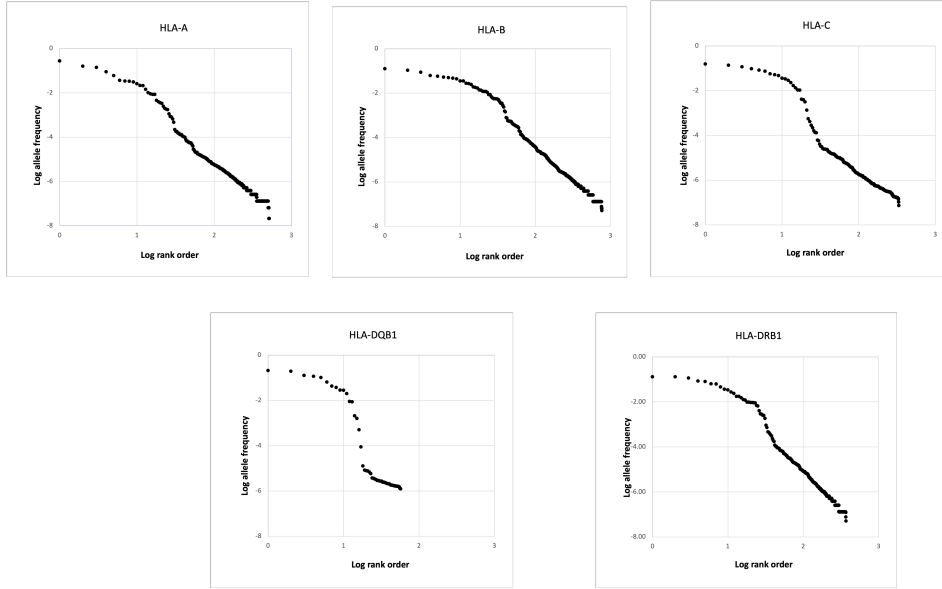


Figure 5: HLA allele frequencies plotted against rank on logarithmic co-ordinates for the five loci that make up the HLA-A~B~C~DRB1~DQB1 Caucasian 5-locus haplotype dataset. All data from the Caucasian allele files were assembled by the US NMDP and are available as separate files from their website.

The results support the proposition that the population on the right-side of the minimum represents haplotypes under positive selection whereas that on the left-side represents those haplotypes subject to drift or negative selection. They are consistent with the conclusions in [5] that linkage disequilibrium is positive ($D'_{ij} > 0$) in high-frequency haplotypes and negative ($D'_{ij} < 0$) among rare haplotypes, and the evidence that the Ewens-Watterson test for homozygosity shows excess homozygosity for common 5-locus haplotypes.

The value of hn in the minimum is about 1020, or rank 1730. Although the two exponentials extend on either side of this minimum, it is useful to denote rank 1730 as an approximate transition point t in the rank order. This point produces an $\approx 80:20$ split in the census population, with those haplotypes under selection ($\approx 80\%$) being the majority by census.

3.2 Log-log rank-frequency plots: HLA class I and II alleles

Data for allele frequencies are derived by the US NMDP directly from their haplotype dataset and shown in the 5 panels of Fig. 5.

HLA alleles do not follow a power law distribution. Rather, their distributions show a relatively small number of alleles that break away from a trend-line for the frequencies of low-frequency alleles. The discontinuity is obvious for HLA-C and HLA-DQB1 but is present at all loci. Reasons why the discontinuities occur is discussed shortly. High-frequency alleles show

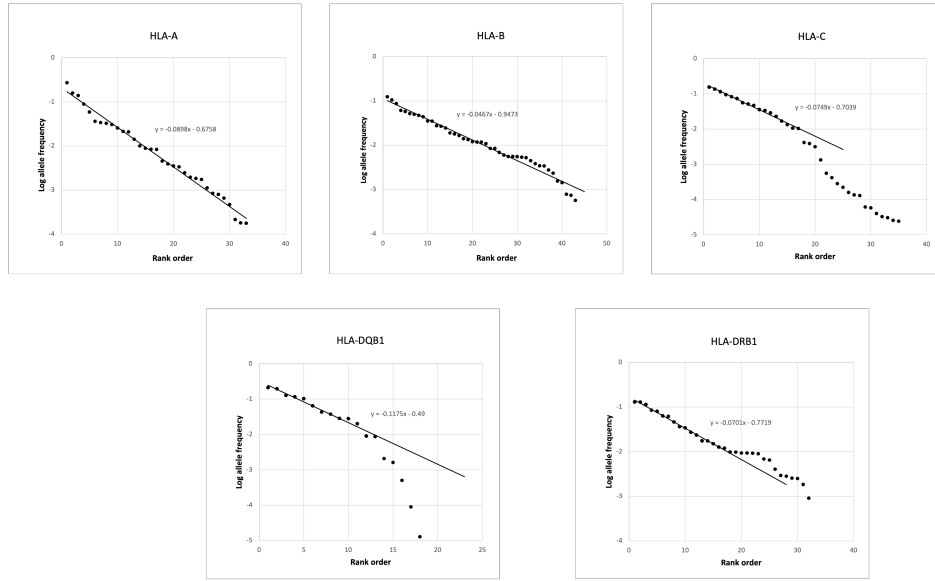


Figure 6: The data used for Fig.5 but plotted here on a linear scale for rank. The data show remarkable linearity for frequencies of numerically lowest rank.

logarithmic decay, as shown by plotting the data in Fig.5 on log-normal co-ordinates (Fig.6). The plots in Fig.6 indicate a geometric decline for high-frequency alleles in which each allele in ascending rank occupies a fixed fraction of the available population after deducting the allelic frequencies of lower rank.

This was an unexpected result, not least because the frequency values for the lowest ranked alleles are themselves composites of many hundreds of separate contributions from each haplotype species to which the allele in question contributes (see evidence below, subsection 3.3). The underlying orderliness of the logarithmic distribution suggests a form of niche allocation, potentially produced by density-dependent capping of alleles. The numbers of alleles identified for each locus in the high-frequency category, together with their cumulative frequencies, are: A/30/0.997; B/40/0.986; C/20/0.996; DQB1/15/0.999; DRB1/31/0.993, making 137 alleles in all. Permutations restricted solely to this group of 137 alleles account for $\approx 97.1\%$ of all haplotypes in the census sample.

The shapes of all five distributions in Fig.5 are similar to that in Figure 2B in the Neher-Shraiman paper [25] (discussed in 2.7 above). However, the two graphs plot different measurements. The ordinate in the NS paper measures estimates of linkage disequilibrium (LD) whereas it is allele frequency in Fig.5. The abscissa in the NS model is crossovers per chromosome but is rank order in Fig.5. Despite these differences, the two plots share commonality.

The starting point for the NS analysis is a group of polymorphic loci [25]. Under Quasi-Linkage Equilibrium (QLE), the potential for emergence of positive epistasis between allelic combinations is frustrated by high rates of recombination. As the recombination rate is lowered, there is a recombination rate below which allelic combinations remain intact long enough

for selection to switch to the haplotype. Competition between the various haplotypes then follows and one haplotype emerges by competitive exclusion.

We assume, as a starting point, that the abscissæ in Fig.5 do not represent a range of recombination rates; rather there is a single recombination rate that is below the critical value identified in [25]. Instead, we regard those alleles to the right of the respective discontinuities as incapable of generating positive epistatic interactions. By contrast, the 137 alleles to the left of the discontinuities do show positive epistatic interactions. We show below that high-frequency alleles contribute extensively to numerous haplotypes in both populations identified in Figs.4a,b. Their frequencies are pulled up by selection on high-frequency haplotypes that contain them. Recalling Eq.11, the fitness of these alleles has both epistatic and additive components and the overall frequency of a particular allele is the sum of the haplotype frequencies to which it contributes is

$$f(A_x) = \sum_1^{i_t} f(H_{A_x})_i + \sum_{i_t+1}^{i_{max}} f(H_{A_x})_i \quad (15)$$

The frequency of allele x is the sum of the frequencies of haplotypes that carry the allele. These haplotypes are partitioned between those of high frequency (that is, low rank) that show the outcome of positive epistasis (first term on RHS of Eq.16) and those of low frequency (high rank) that are neutral or deleterious (second term on RHS of Eq.16). The composite allele frequencies are those for haplotype rank i , and the transition point occurs at rank i_t . We propose the data points in the five panels in Fig. 5 to the left of the discontinuities are those whose overall frequency has both components of Eq.11, whereas those to the right have no epistatic component. Viewed in this light, the ordinates in Fig.5 are log frequencies, $\log f(A_x)$, that include additive components and, in some cases, an additional epistatic component.

We have built on this approach to gain an approximate measure of the positive epistatic effect that provides the basis for additional selection in high-frequency haplotypes. The results are shown in Fig.7. By splitting the frequency of individual alleles into a component that only arises in high-frequency haplotypes, we gain access to $A + E$ for a particular allele. The frequency gap between the two lines represents an approximate measure of the positive epistasis, and this appears as an increase in linkage disequilibrium. Convergence of the two lines gives an assessment of the point at which positive epistasis ceases to emerge, allowing us to identify the 137 alleles around which an HLA network or cloud emerges.

We are now in a better position to see why there should be a similarity between the plots in Fig.5 and that in Figure 2B of Neher and Shraiman [25]. The ordinate in the NS paper is log-linkage disequilibrium (LD) and is log-frequency in Fig.5. The two are connected because the highest allele frequencies reflect positive selection on the haplotypes that contain them, and positive epistasis and low recombination rates are the basis for the LD shown by major haplotypes. The discontinuities in Fig.5 represent the point at which there is no epistatic contribution to lower allele frequencies.

3.3 Interim assessment I

The evidence, so far, is consistent with two distinct haplotype populations (Figs.4a,b). One population accounts for at least 80% of the haplotype census population, and we suggest this

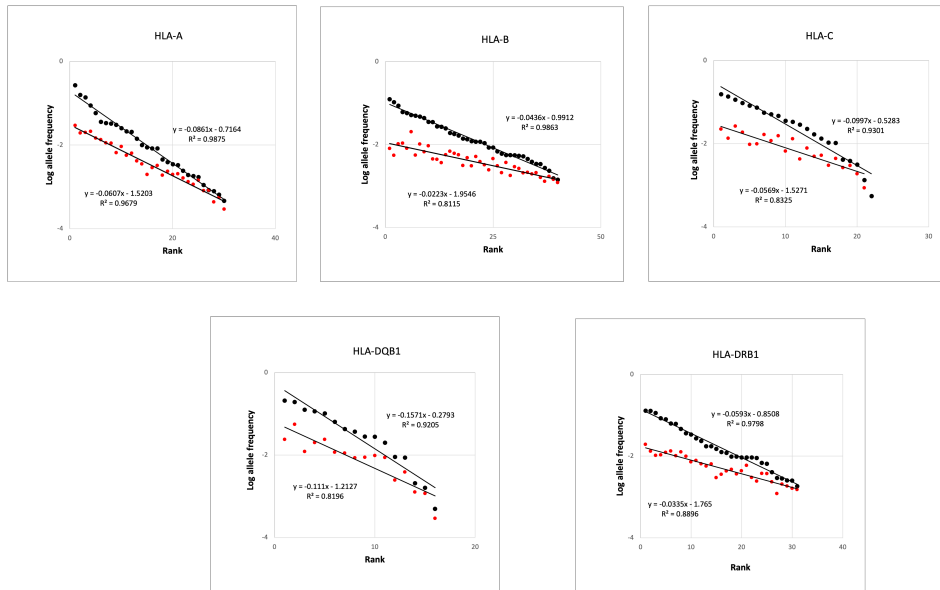


Figure 7: Data as in Fig.6 (black markers), limited to allele frequencies above the discontinuities shown in Fig.5. Red markers indicate residual allele frequencies after deduction of a frequency component attributable to positive epistasis, E , as defined in [47]. Somewhere between 9 and 12% of the highest frequencies at each locus is attributable to the heritable component, A .

population is under different degrees of positive selection. The second population consists of low-frequency haplotypes that are either neutral or mildly deleterious. The allele frequency data are consistent with the elevation of a cohort of 137 alleles to substantial frequencies due to positive epistasis at haplotype level, leading these haplotypes to come under purifying selection. We attribute the orderly spread, both of haplotype and allele frequencies, as indicative of an HLA system whose components are held at intermediate frequencies due to density-dependent effects on growth. The obvious external agency for density-dependent host population regulation is disease transmission.

We can also begin discussion of stability of haplotype distributions as complex systems. The two layers, haplotype and allele, have some properties of trophic layers but can be recognised as having different general characteristics. The haplotype layer is characterised by a large number of individual haplotypes (somewhere between 350 and 1850) whose combination in diploids is continually broken up by segregation. The number of effective alleles is much smaller per locus, with mutualism restricted to specific allelic combinations. It is worth quoting May [50] at this point:

“Roughly speaking, this suggests that within a web species which interact with many others (large C) should do so weakly (small α), and conversely those which interact strongly should do so with but a few species. This is indeed a tendency in many natural ecosystems, as noted, for example, by Margalef⁷: “From empirical evidence it seems that species that interact feebly with others do so with a great number of other species. Conversely, species with strong interactions are often part of a system with a small number of species ...”

The reference to Margalef is page 7 in [56]. The sense of May’s statement is improved by the insertion of a comma between *web* and *species* in the first sentence. May’s paper “Will a large complex system be stable?” has been profoundly influential (see introduction to [51], for example). “The notion of stability referred to by May and these later works is that of asymptotic linear stability of an equilibrium point” [51]. That notion is core to the approach in this paper, although it should be noted that the haplotype cloud that emerges from the data will not be that of a random matrix. At this point, we would note that in the two trophic layers mentioned in the first paragraph of this section, that containing the haplotypes have large connectedness (large C) and weak interactions (small α), whilst the allele layer has the opposite: low connectedness and strong interactions.

The remainder of this Results section is taken up with detailed evidence to support the conclusions reached so far.

3.4 Allele spreads across 5-locus haplotype distributions

This subsection looks specifically at the spread of class I and class II alleles across the NMDP Caucasian 5-locus haplotypes. The purpose of the analysis is the better to understand allele distribution across the haplotype board for single alleles identified from Fig.5 as potentially under positive epistatic selection. Alleles at all five loci were examined. These frequencies are taken from the slightly truncated lists available from the NMDP website.

The data presented here are for four of the 137 alleles identified earlier. The difference in rank, in all four panels, between two adjacent appearances of an identified allele in the

ranked list of HLA haplotypes, is plotted linearly on the y-axis against the rank position of the first allele of the pair. Every data point represents a different haplotype. The results are shown in Fig.8 for (a) A*02:01g, (b) DRB1*07:01, (c) A*01:03g, and (d) DRB1*04:13 as representative distributions. Panel (a) shows the most frequent class I HLA-A allele, A*02:01g and (b) the most frequent class II HLA-DRB1 allele, DRB1*07:01. These two alleles are components of many hundred haplotypes each. That is, they are highly pleiotropic (for fuller discussion of pleiotropy, see [57]). Those alleles under selection constitute no more than the first 2000. Panels (a) and (b) therefore demonstrate the extensive involvement of both alleles in haplotypes that are subject to drift. The average rank difference is 5.3 for the top 5000 haplotypes containing A*02:01g and 9.3 for DRB1*07:01. By contrast, the average for haplotypes of ranks from 32,000 to 37,000 is 8.4 and 14.4 respectively. This indicates a degree of interpolation at low frequencies by mutant alleles that are individually rare but numerous in aggregate.

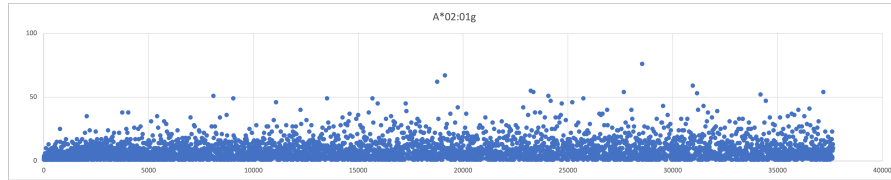
Panels (c) and (d) have an extended linear scale on the ordinate (x40 that in the first two bands). Allele A*01:03g (c) has rank 31 in the HLA-A catalogue, which places it at the discontinuity in the HLA-A panel of Fig.5. Allele DRB1*04:13 (d) has a rank of 75 and places it in the portion of the HLA-DRB1 panel in Fig.5 whose alleles show no epistatic component of fitness. These two lower panels are characteristic of less frequent alleles, showing little or no presence in the first 5000 alleles by frequency.

The two major alleles contribute extensively to minor haplotypes, certainly down to rank 37,000. We should recall that the minimum in Fig.5(a) is located between ranks 1000 to 2000, emphasising that the spectra in the panels in Fig.8 are dominated by the low end of the frequency spectrum. Panel (c) for A*01:03g, which has the lowest frequency of the HLA-A alleles above the discontinuity in Fig.5, shows that the distance between successive allele appearances is initially much greater than for a high-frequency allele such as A*02:01g, before settling into a more regular pattern of rank separation.

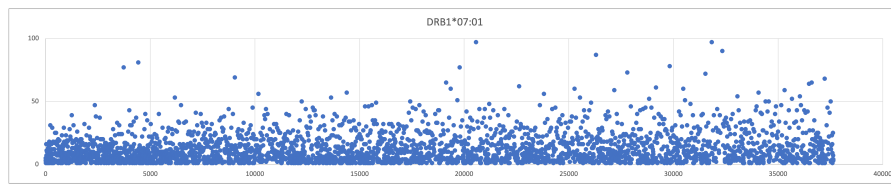
The overall number of haplotypes by census population associated with mutant alleles is <3% of the total census population size, where a mutant is an allele that is not one of the 137 alleles identified earlier. Since the census haplotype population to the left of the minimum in Fig.4a is $\approx 20\%$ of the total, most of the haplotypes by census population in this 20% do not contain mutants; rather, they are permutations of the 137 alleles but without generation of positive epistasis. This suggests, in turn, that the additive component of fitness in most haplotypes is intrinsically low.

3.5 Distribution of epistatic effects

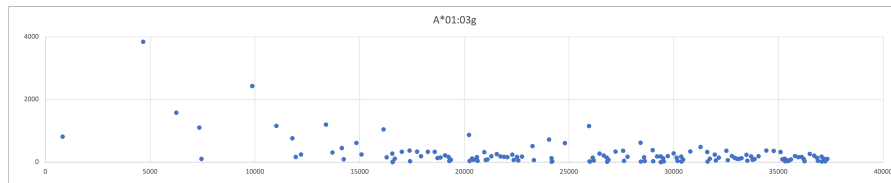
Fitness is higher in some haplotypes but not others due to the uneven distribution of positive epistasis. This can be demonstrated by looking at the frequencies of haplotypes derived from the top 5 class I alleles (-A, -B, -C) by frequency. There are 125 possible permutations and all 125 are found in the NMDP CAU catalogue. The results are shown in Fig.9a. The red markers indicate the actual frequencies of the 125 class I haplotypes on a logarithmic scale. The black markers indicate the calculated frequencies of the 125 possible class I haplotypes obtained as the product of the actual frequencies of the individual alleles. The calculated frequency values sit in a band that is approximately one order of magnitude wide. By contrast, the actual frequencies span approximately 5 orders of magnitude. One interpretation is that the right-



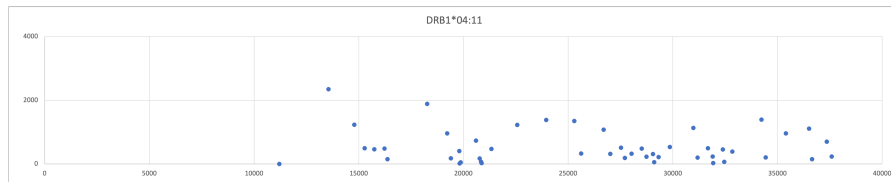
(a) A*02:01g



(b) DRB1*07:01

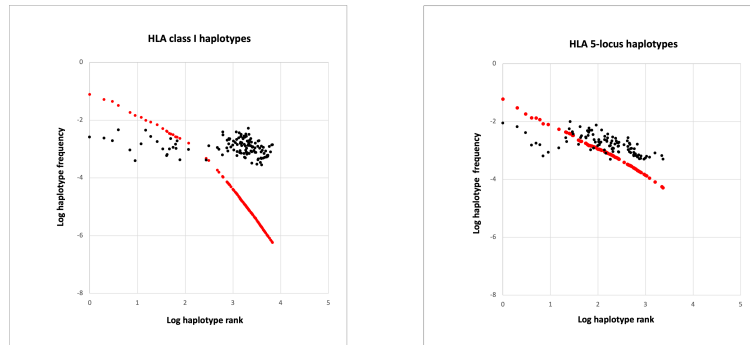


(c) A*01:03g



(d) DRB1*04:13

Figure 8: Allele spreads across ranked haplotypes. Ranks run from 1 to 37,000 in all four panels.



(a) Results for randomisation of the highest frequency class I alleles (top 5 alleles for -A, -B, and -C loci), generating 125 possible class I haplotypes. All haplotypes are represented in the NMDP sample. Calculated haplotype frequencies (black); actual haplotype frequencies (red). The plot shows that randomisation of alleles has limited effect on calculated haplotype frequencies. Actual haplotype frequencies, by contrast, are widely spread, indicating the existence of a recombinational load.

(b) Results for randomisation of the highest frequency class I and class II haplotypes (top 10 each), generating 100 possible 5-locus haplotypes. Calculated 5-locus haplotype frequencies (black); actual 5-locus haplotype frequencies (red). The plot shows that randomisation of class I and II haplotypes has limited effect on calculated 5-locus haplotype frequencies, but a marked effect on actual haplotype frequencies. The plot shows that randomisation of alleles has limited effect on calculated haplotype frequencies. Actual haplotype frequencies, by contrast, are widely spread. The effect is less marked than in (a).

Figure 9: Plots of log haplotype-frequency against log haplotype-rank.

hand cluster of theoretical frequencies is characterised by HLA class I haplotypes that are of low frequency and not subject to selection. The haplotypes of interest are the 21 haplotypes on the left-hand side. These are under positive selection if assumptions about steady-state or quasi-steady-state nature of haplotype frequencies are accepted. These 21 haplotypes are still spread over two orders of magnitude and reflect steady-state fitnesses accordingly.

The conclusion of interest is that randomising the alleles in the class I haplotypes of highest frequencies uncouples the positive epistasis seen in a minority of allelic combinations. It demonstrates at first hand the cost of the recombinational load.

A similar effect can be seen in combinations of class I and II haplotypes (Fig.9b). This figure shows the outcome when the top 10 haplotypes of each class are used. These give an overall set of 100 possible 5-locus haplotypes, again all of which are in the NMDP Caucasian datasets. The spread of actual haplotype frequencies is noticeably smaller, at three orders of magnitude. This plot of 5-locus haplotypes can be mapped directly to Figs.4a and b, and covers the range of haplotypes under selection. This should not be surprising, since the contributing class I and II haplotypes are all under selection themselves. Despite this preselection, the evidence suggests that randomisation of class I and II haplotypes generates a range of steady-state fitnesses, subject to qualifications that have already been discussed.

It should be noted that the calculated frequencies in both Figs.9a and 9b reflect constituent

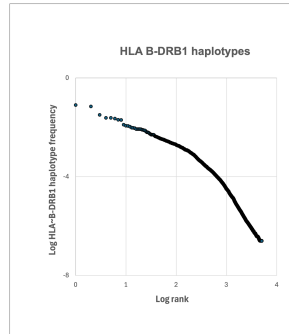


Figure 10: Frequencies of Caucasian HLA B-DRB1 allele pairs plotted against rank on logarithmic co-ordinates

allele frequencies that are elevated through their presence in haplotypes showing positive epistasis. The calculated frequencies for haplotypes using allele frequencies that are devoid of any involvement in epistatically-selected haplotypes would be lower.

3.6 Further evidence of linkage

The data in the previous section provide evidence that the positive epistasis evident in high-frequency HLA haplotypes is not simply due to random combinations of high-frequency alleles. Rather, the epistasis arises from specific combinations. This is no surprise. Evidence published in 2013 [16] provided evidence of non-random association of HLA class I and II alleles, citing work on two relatively isolated populations, the Burusho population of Pakistan and the Hutterite population of South Dakota in the US [16]. An important part of that paper addressed the issue of recombination between class I (beta block) and class II (delta block) alleles, since these are separated by the gamma block, with a known possibility of recombination between the blocks. Evidence of coupling between B and DRB1 alleles supported a model in which selection on discrete allelic combinations was maintained by pathogen interactions with hosts.

We tested the ability of the much larger NMDP Caucasian dataset for evidence of long-range associations, focusing here on the results for HLA-B~DRB1. Fig.10 shows the frequency of HLA-B~DRB1 pairs plotted against rank, both on logarithmic co-ordinates. It has the same broad shape as the 5-locus haplotype distribution of Fig.3, but the linear portion of the distribution is limited to the first ≈ 150 pairs by rank, out of a possible number of 1240 ($= 40 \times 31$) pairs. Possibly 250 pairs in total, or 20%, could be considered as being under selection.

A frequency plot of the top 18 HLA-B alleles by frequency against the top 15 HLA-DRB1 alleles is shown in Fig.11, with coloured bars indicating their frequencies. The frequency associated with each allele pair is itself an aggregate, because the contributing alleles are pleiotropic. The data indicate two major pairings, B*08:01g/DRB1*03:01g and B*07:02/DRB1*15:01, and about 10 moderate pairings, out of the ≈ 250 under selection.

The two major allele pairs account for $\approx 8\%$ and $\approx 6.9\%$ of the HLA-B~DRB1 popula-

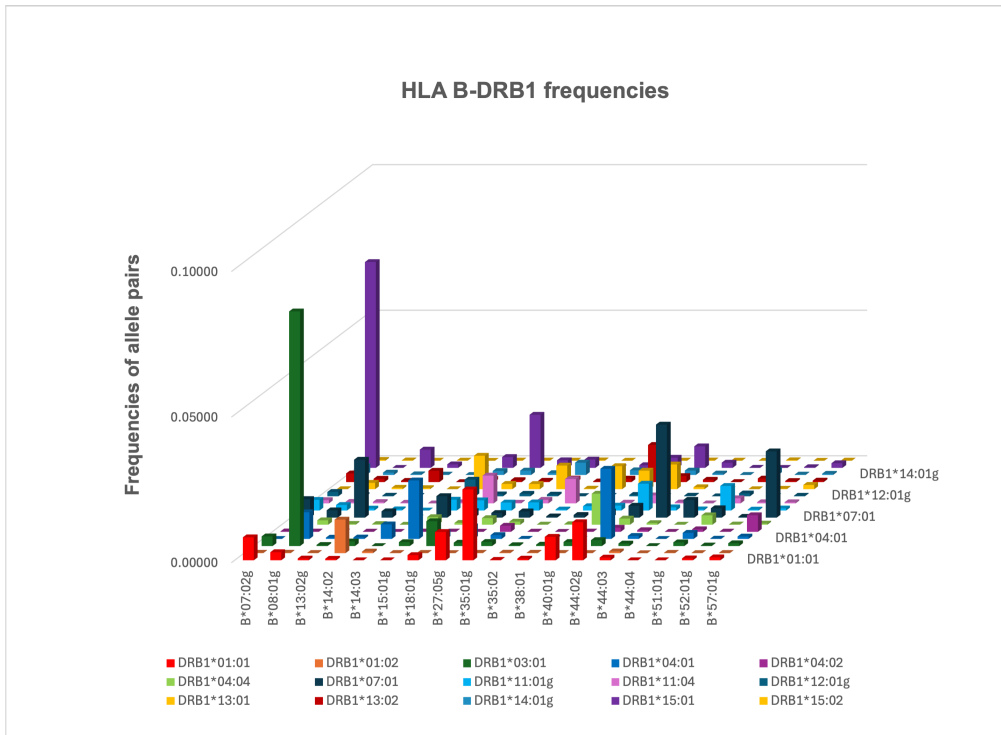


Figure 11: Frequency distribution of HLA-B~DRB1 pairs; The two loci are separated by a potential recombination region in the wider HLA locus. The data suggest the region has the ability to set recombination at a sufficiently low level for selection on positive epistasis and linkage disequilibrium.

tion respectively. Common HLA-B~DRB1 pairs are associated with high-frequency 5-locus-haplotypes.

3.7 Interim assessment II

The data presented so far provide evidence of selection on haplotypes, with major haplotypes benefiting from positive epistasis. This epistasis arises from specific interactions between the 137 alleles from the five transplantation loci that show demonstrable effects on their frequencies from an epistatic component. There are ≈ 11.1 million possible permutations of the 137 alleles of which 350-1850 are under selection. The precise boundary is difficult to determine because the tail of those under selection overlaps with the population behaving neutrally or under mild negative selection. Those under selection account for $\approx 80\%$ of the census population, whilst further permutations of the 137 core alleles account for a further 17%. There is then the remaining 3% of haplotypes by census that represent haplotypes with one or more alleles that lie outside the 137. These alleles are mutations. Many of the haplotypes that are not under selection may have functional value, not least in diploids, by interposing further hurdles to avoidance of presentation [58].

The picture that emerges is a core network or community of highly related molecular species. The high level of relatedness directly reflects the pleiotropic properties of the higher frequency alleles.

3.8 Mapping core HLA class I alleles onto HLA supertypes

A key consideration in considering community structure is its stability. Of direct interest, therefore, is evidence that some major HLA alleles show longevity that exceeds the generation times of most pathogens by orders of magnitude.

A major computational analysis of 10,956 distinct HLA class I allele DNA sequences (HLA-A, 3489; -B, 4356; and -C, 3111) was published in 2017 [8]. The data pointed to two origins for the variation between alleles at each of the three loci: single nucleotide polymorphisms (SNPs) and recombinational events. Alleles with SNPs differ by point mutation from older, more common alleles. Removal of these SNP-carrying alleles from the set of 10,956 revealed a residue of 1171 allele types related to each other by recombination (-A, 236; -B, 775; -C, 160). Removal of these alleles, in turn, revealed a set of 42 core allele types (-A, 11; -B, 17; -C, 14) that represent all functionally significant variation in exons 2 and 3 that cannot be derived by recombination events and point mutation. They are regarded as older in their origins than either the SNP alleles or recombinant alleles, and approximately half of them by census fraction are consistent with Denisovan or Neanderthal origins.

An older classification of HLA class I alleles has been into supertypes [12, 59]. A recent update of supertype classification uses an approach based on structural similarity [13].

These two classifications can be combined with the class I allele frequency distributions shown in Fig.5 to identify the relationship between the antiquity, the lack of relatedness, and the frequency of particular alleles. The results are shown in Figs.12-16. Fig.12 shows the principal supertypes identified in [13] as headers of each column, and the ordinate shows the rank order of each allele. Blue represents core alleles as identified in [8] of potentially Neanderthal/Denisovan origin, orange represents remaining core alleles, and green represents

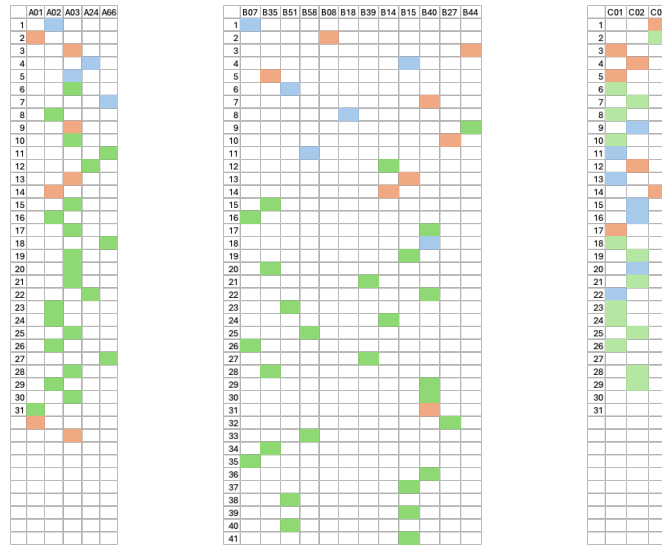


Figure 12

alleles of more recent origin that are related to the core alleles. Two additional entries in the data for class I HLA-A alleles for ranks 32 and 33. Gaps at the lower levels of class I HLA-C alleles reflect the absence of these alleles in the supertype catalogue list. All three class I loci are represented at the highest allele frequencies by core alleles as identified in [8], but there are subtle differences.

We have visualised frequency distributions for each supertype in Figures 14-16.

The current position on the temporal origin of these alleles appears currently to be the following. The Neanderthal split from the common ancestor of modern humans occurred about 530 kya and from Denisovans about 400 kya. Modern humans arrived in Europe in an out-of-Africa migration, passing through a bottleneck that is thought to have eliminated Neanderthal/Denisovan ancestry as it migrated. The Neanderthal DNA that exists in modern Caucasian populations is considered to have arisen in a subsequent period of reproductive contact that occurred about 45-50 kya. Neanderthals went extinct about 40 kya, preventing more recent introgression. The level of Neanderthal introgression from 50 kya is thought to have been $\approx 10\%$ of the Caucasian genome, abating to its current level of an average of $\approx 2\%$ through conventional purifying selection. However, modern Caucasians have a frequency of Neanderthal/Denisovan HLA alleles that is higher than 10%. These frequencies are thought to represent positive selection for alleles that are better adapted to local pathogens. There appears to have been sustained survival of alleles of Neanderthal/Denisovan allele candidates at A and B loci.

An important modification to this view is that positive selection acts on haplotypes. High-frequency haplotypes acquire fitness through positive epistatic effects between alleles. Allele frequencies are high where epistatic effects across multiple haplotypes leads to frequency aggregation at the allelic level. Alleles are themselves regulated by the same negative-dependent

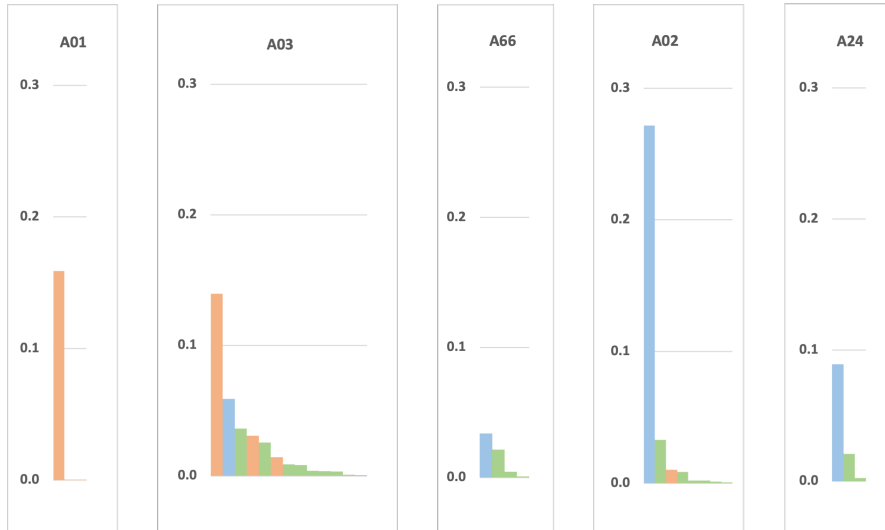


Figure 13: Frequencies of major *HLA-A* allele distributed into their respective supertypes (as defined in [13]). Blue represents core alleles as identified in [8] of potentially Neanderthal/Denisovan origin, orange represents remaining core alleles, and green represents alleles of more recent origin that are related to the core alleles.

disease transmission factors that also regulate haplotype frequencies. Adaptation to local pathogens is likely to be reflected in nuanced shifts in haplotype frequencies that are then reflected in changes in allele frequencies.

The existence of Class I supertype silos is strong evidence of niche apportionment through limiting similarity, an expected outcome from the model we have proposed. The existence of a major allele in many HLA-A and -B silos is consistent with competitive exclusion within the boundaries of those silos. It may also be that the classification into supertypes requires further refinement, as multiple alleles within a single allelic silo may represent different epistatic properties.

There is also longstanding evidence of even longer survival of HLA class II alleles, as evidenced by *trans*-species polymorphisms. The most recent separation of humans from apes was that with chimpanzees between 7 and 9 million years ago [60], or about 250,000-300,000 generations ago.

One obvious explanation for the longevity of major class I and II alleles is that they represent those with high long-term fitness. This fitness is generated by their ability to enter numerous positive epistatic relationships with alleles from other HLA loci. Although it is difficult to date core alleles that are not of Neanderthal/Denisovan origin, there is no reason why they should not be a legacy of the out-of-Africa migration population that met the incumbent Neanderthal population in Western Europe some 45,000 years ago. However, this remains to be demonstrated. Second, it might be argued that supertype silos, such as A03, B40, B44, C01, C02, and C03, where more recent alleles are present at considerable frequencies are evidence



Figure 14: Frequencies of major *HLA-B* allele distributed into their respective supertypes (as defined in [13]). Blue represents core alleles as identified in [8] of potentially Neanderthal/Denisovan origin, orange represents remaining core alleles, and green represents alleles of more recent origin that are related to the core alleles.

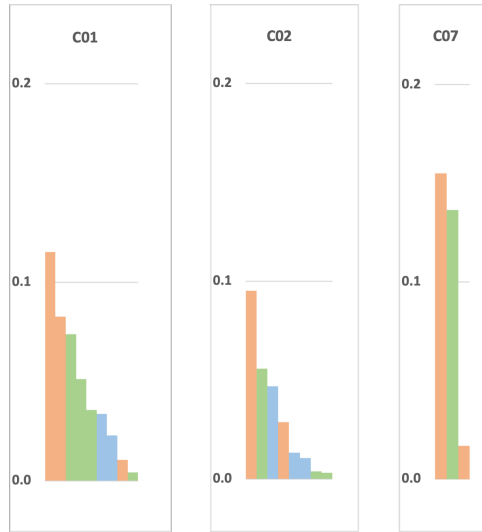


Figure 15: Frequencies of major *HLA-C* allele distributed into their respective superotypes (as defined in [13]). Blue represents core alleles as identified in [8] of potentially Neanderthal/Denisovan origin, orange represents remaining core alleles, and green represents alleles of more recent origin that are related to the core alleles.

of changes in frequency that are under way. That possibility has to be set against two other factors: (i) the survival of ancient alleles in the face of ongoing attempts by pathogens to avoid HLA peptide presentation, particularly by viruses, and (ii) the evidence that allele frequencies can be used to track human migrations, suggesting that a degree of frequency stability is possible even in the face of disease. If frequencies generally are stable, then wild fluctuations that fully dislodge alleles would seem less plausible. Indeed, the only major selective sweep leading to elimination of a class I supertype for which there is good evidence is the loss of A*02 in west-African chimpanzees [61]. This has been attributed to the emergence of a devastating Simian Immunodeficiency Virus (SIV).

4 Discussion

4.1 HLA haplotypes form a large inter-connected network

The extent of the polymorphism associated with the HLA transplantation loci has emerged progressively over the past 8 decades or so. It is now recognised as very extensive. Two of the principal explanations for the polymorphism are also longstanding: negative frequency-dependent selection (NFDS) and heterozygote advantage (HA). They focus on alleles, not haplotypes, and they assume open-ended population growth as envisaged in Fisher's Fundamental Theorem of Natural Selection. Fisher's association of fitness with the rate constant for exponential population growth is an in-built assumption of these models, with non-existent

consideration of Fisher's Malthusian parameter and its attenuation to zero with increases in population density. Both NFDS and HA mechanisms require similar fitnesses to sustain multiple alleles or heterozygotes and to avoid competitive exclusion. This is at odds with evidence of widespread differences in frequency that are at least quasi-stable, itself supported by evidence of substantial linkage disequilibrium in major HLA haplotypes.

We propose a substantial departure from these assumptions. At the evidential level, there is support for the view that it is HLA haplotypes that carry a major part of the selective burden, not the allele. In addition, the problem of achieving zero effective fitness of haplotypes is attributed directly to the density-dependence of pathogen transmission. There are sufficient human pathogens to allow approximately 1500 agencies to determine the number of HLA haplotypes. Collectively, the haplotype network drives selection of the 137 HLA alleles whose pleiotropy drives the epistatic effects that underpin the network. The orderly behaviour of both haplotypic and allelic frequencies suggests the network itself is under selective pressure. In this respect, it would have some of the properties of a quasi-species.

This model has a number of implications. First, there are the evolutionary ones. The focus in heterozygote advantage was a beneficial expansion of the range of peptide recognition in diploid individuals through possession of two functionally-distinct alleles in *trans* at each locus, a direct consequence of diploidy. This pairing is random, and associations are broken up in meiosis. Haplotypes, by contrast, survive numerous rounds of segregation and meiosis, and demonstrate substantial positive epistasis and linkage disequilibrium. Complementation is undoubtedly important for overall HLA function, but it manifests itself in *cis*, not *trans*. This looks to be an evolutionary adaptation.

If so, we should look at the way that peptide binding operates across the haplotype as a whole. This binding can be represented as $pHLA_{haplo}$ rather than $pHLA_{allele}$. As far as we know, HLA molecules are not coupled physically on the peptide-presenting cell, but co-presentation on cell surfaces potentially provides a form of coincidence detection in the target T-cell response for the 12 (=2x6) distinct HLA alleles used by a diploid host. In pursuing this goal, we should keep a watchful eye on the downstream consequences of presenting numerous peptides to individual T-cells from 12 different HLA molecules. There is, for example, an interesting case in which there is linkage between two alleles in the DR region, the DR2 haplotype, where one allele modifies the response of the other through activation-induced cell death [62]. The allelic pairing offers partial protection against multiple-sclerosis-like disease. Given the evidence that numerous diseases are associated with the broader HLA region of chromosome 6, distinctive interplay between alleles of the HLA transplantation loci can be expected on a significant scale.

Focus on the behaviour of major alleles and haplotypes does not mean that rare HLA haplotypes are without utility. A useful account of their potential can be found in [58]. The evidence that most of the alleles by census in rare haplotypes are derived from the 137 identified earlier (17% out of 20%) indicates that rare haplotypes will be functional, even if there are too few to demonstrate epistatic effects. In this respect, rare but functional haplotypes will continue to complicate the challenges presented to pathogens by individual hosts. This will be particularly important during reproduction since it produces distinctively different HLA genotypes within members of the same family. These have historically lived in close proximity in small tribal communities. Diploidy and sexual reproduction would provide an acute protective benefit at the HLA locus, coupled with additional effects through independent assortment of

other polymorphic sites involved in the adaptive immune response, such as the KIR locus on chromosome 19.

The model we propose conforms in broad outline to that predicted by Margalef [56] and May [50] for stable communities. In the case here, the allelic interactions in HLA haplotypes are strong and the number of alleles involved is small (large α , small C), whereas interactions between haplotypes are weak and haplotypes are numerous (large C , small α).

4.2 Stable networks, Red Queens, and Enigma machines

The previous section cited some of the reasons for network stability. The major alleles show evidence of longevity: putative evidence of Neanderthal/Denisovan origins for class I, and trans-species polymorphism (TSP) for class II. Additionally, the evidence of strong linkage disequilibrium implicitly requires stability for the positive selection to manifest itself. Selective positive epistasis generates a recombinational load from breaking up successful haplotypes. The physical compactness of frozen haplotypes limits the sites for recombination and recombinational rates are lower in many cases than that for the genome as a whole [63, 14], although there is considerable variation between haplotypes [64]. The emergence of positive epistasis and sharp increases in linkage disequilibrium are contingent, on the NS model [25], on recombination rates that fall below a critical value.

It greatly assists the theoretical analysis if the network is treated as stable over the short term, since frequencies become measures of fitness (section 2.4 of this paper). Many of the graphs become readily interpretable on that basis.

However, the existence of haplotypes with medium-to-long-term stability appears to sit uncomfortably with the rapid reproduction rates of many pathogens and their ability to sustain high mutational loads. Rapid mutation of pathogens provides an opportunity for them to probe for weaknesses in slowly-adapting host defences, setting up an apparently one-sided chase between rapidly-reproducing predator and slowly-reproducing prey. This scenario differs markedly from conventional predator-prey relationships, characterised by the Lotka-Volterra predator-prey equations, where the predator reproduces more slowly than the prey.

The successful resistance to pathogens offered by human hosts through the adaptive immune system has two components: presentation of pathogen-derived peptides by HLA molecules followed by rapid amplification of the presentation response through T-cell activation.

The parallel between the reproductive properties of pathogens and that of the amplified response in humans can readily be seen in antibody production, where responsive antibody-producing cells reproduce and diverge rapidly through clonal expansion and hypersomatic mutation of antibody candidates. High-affinity antibodies are selected by affinity maturation. Pathogens such as *Plasmodium falciparum* (malaria) and *Trypanosoma brucei* (trypanosomiasis), for example, provide text-book examples of bait-and-switch played on the human antibody response that are pure Red Queen. They show that human hosts do have defensive responses that match rapidly-reproducing pathogens in speed.

By contrast, the challenge faced by the host presentation step is that it remains unchanged for the lifetime of the human host, with a generation interval that is 3-4 orders of magnitude slower than many pathogens. That stability allows removal of self-reactive T-cells during foetal development, with the survivors sensitive to exogenous peptide. But it makes pathogen avoidance of peptide presentation an eminently achievable goal; or so it appears. The evolutionary

response that frustrates pathogen breakthroughs through this static defence is to balkanise host presentation of pathogen-peptide by generating a large network of presenting haplotypes.

Conceptually, it follows closely the use of Enigma machines in WWII. The starting rotor positions for the three slots in the machine were set each morning according to a cypher manual printed month's in advance. The rotors carried 26 'letters' and the ensuing encryption was considered to be unbreakable. Alan Turing realised that the encyphered messages could be broken if all possible daily settings could be scrutinised quickly. The search would be successful if a setting was discovered that could produce readable German text. Turing developed an electro-mechanical device (improved by Welchman) that greatly reduced the time needed to break a daily setting.

The construction of an Enigma machine with slots for three rotors to operate together has an obvious parallel in multi-locus HLA haplotypes, where each rotor contains 26 letters that parallel HLA alleles. By analogy, the electro-mechanical device was the pathogen, canvassing rotor permutations in the hope that one would open up the rotor settings for the day. Since distribution of Enigma messages was effectively clonal, successful decoding resulted in a sharp increase in decoded information.

Enigma security was progressively improved during the course of WWII through introduction of a fourth slot and additional rotors. This is paralleled by increasing haplotype size. The size of the information gain for each breakthrough was reduced by partitioning of daily settings into different groups. This reduction in decryption success is directly paralleled by polymorphic HLA genotypes.

The design of the Enigma machines, and the history of their cracking has clear messages for a biological peptide-presentation device such as HLA haplotypes that pathogens wish to avoid. One strategy is to increase the range of problems that pathogens face when they are degraded and presented. A coupled set of HLA loci in close physical proximity, as in a haplotype, allows for selection on allelic complementarity between different alleles, making simultaneous avoidance challenging for pathogens. The challenge of avoidance is increased by making HLA molecules act as broad-spectrum, low affinity binders of peptides. Thus the dissociation constants of HLA molecules are typically in the μM -nM range. By contrast, antibodies are high-affinity, narrow-spectrum binders with dissociation constants typically in the nM-pM range. They are much easier to avoid using bait-and-switch. Finally, doubling the number of HLA species in every host through diploidy, with each peptide-presenting cell carrying 12 different HLA alleles.

A second strategy is to limit the damage caused by pathogens by ensuring that hosts they might infect are different from ones that have previously shown susceptibility, an example of the benefits of genetic rarity, both in parallel and in series.

There are also important differences between pathogens and Enigma coding. For example, the Enigma system has no obvious benefit in selection for some rotor settings over others, or positive epistasis.

Haldane canvassed the view that "*it is an advantage to the individual to possess a rare biochemical phenotype. For just because of its rarity it will be resistant to diseases which attack the majority of its fellows.*" Later in the same paper, he expressed the view that: "*We have here, then, a mechanism which favours polymorphism, because it gives selective value to a genotype so long as it is rare. Such mechanisms are not very common.*" [65]

Haldane was surely right. The limitation imposed by proponents of NFDS was to assume

that rarity has to rest in HLA alleles, whereas it has to rest more widely in the defence genotype taken in the round. The HLA haplotype is an interim stage. The proponents of HA failed to foresee that complementation of HLA allelic function could be brought under tighter genetic control if it occurred within the context of haplotypes. Heterozygotes may indeed enjoy advantages because they make life more difficult for pathogens but it is not the whole story.

4.3 Balancing selection, Fisher's geometric model, and quasi-species

Polymorphism of HLA loci is widely seen as an iconic example of balancing selection [66]. If we are to accept that view, we had better understand what balancing selection means.

The first person to use the term *balancing selection* is unclear. Muller used the term *balancing lethal* in a 1917 paper to describe the outcome of a breeding experiment in *Drosophila melanogaster* [67]. Ford used the term *balanced polymorphism* in 1945 to describe the industrial polymorphism displayed in England by the peppered moth, *Biston betularia* [68]. He distinguished between *transient* and *balanced*, emphasising a high degree of permanence in the ratios of the respective morphs in balanced polymorphism.

We need to recognise two distinct types of occurrences. One is where the two or morphs occupy the same space homogeneously. That is true for human females and males, and the sex ratio is a balanced polymorphism. It is not quite 50:50 for reasons explained by Fisher [69]. The other type of occurrence is where two morphs occupy two distinct regions of a heterogeneous space. This polymorphism is the one shown by industrial melanism [70]. Wild-type peppered moths occupied unpolluted regions to the west of Liverpool and Manchester. The *carbonaria* mutant, which is black and possibly more resistant to air pollution, was prevalent in the two cities in the 19th century, whose trees were covered in soot. The regulatory agent on both moth populations was birds spotting resting moths on trees whose bark coloration varied with the level of pollution. Establishing the density of moth populations is likely to have been technically challenging, and observations relied on catching nocturnal moth samples with light traps and measuring frequency ratios. These inevitably add up to unity, running the risk of giving a spurious semblance of balance. On Levin's principle [41], the two states, unpolluted and black, should be able to sustain two morphs and, to a first approximation, that is what happens - the two moth strains distribute according to their losses by avian predation.

There is a transitional zone to the west of Liverpool where unpolluted trees give way to soot-covered trees. This zone is only 40 km at most on the sampling isocline that runs from west Wales out to the North Sea in the east [70]. The prevailing wind is from the south-west, possibly compressing the zone. It is entirely possible that the zone mid-point is almost entirely depleted of both morphs because both are highly visible on partly-polluted trees. This would potentially establish a third niche for moths that were genetically part way between wild-type and black. It is no surprise, therefore, that three genetic intermediates exist at low frequencies, but there is no useable data on their distribution.

Transferring these ideas to HLA polymorphism, it is clear that some HLA polymorphism might have arisen through spatial differences in the pathogen environment. However, this is a special case. A more general explanation requires an explanation for HLA polymorphism where the environment is complex and the complexity is distributed homogeneously.

A recent summary of the current position of HA and NFDS is contained in the introduction to [71]:

“Two types of balancing selection have been commonly invoked, heterozygote advantage, and rare allele advantage (also called negative frequency-dependent selection). Both heterozygote advantage and rare allele advantage are assumed to result from the role class I and II loci play in the immune system. In general, alleles differ in their peptide-binding regions and hence can present different antigens for inspection by T cells and also regulate natural killer cell activity. Consequently, an individual that can present more kinds of antigens efficiently because it is more heterozygous will likely be able to mount an effective immune response to a larger variety of pathogens. The difference between the 2 hypotheses is, from a population genetics perspective, not very important. In the heterozygote advantage model, heterozygosity at each locus is itself favored by selection because it provides defense against a pathogen pool that is regarded as unchanging. In the rare allele advantage model, an allele in low frequency is favored because pathogens are not yet well adapted to it. As an allele increases in frequency, pathogens adapt and the allele’s contribution to fitness decreases. In the rare allele advantage model, HLA loci and pathogens coevolve in a way that results in higher average fitness of heterozygous individuals. In the heterozygote advantage model, coevolution plays no role. The reason the difference between the models is not important for population genetic analysis is that Takahata and Nei (1990) showed the equations that govern the change in allele frequency to be the same in the 2 models when the allelic fitness in the rare allele advantage model is a linearly decreasing function of frequency. Spurgin and Richardson (2010) provided further support for Takahata and Nei’s conclusion.”

The references in this quotation are to Takahata and Nei [72], and Spurgin and Richardson [73].

This quotation from 2022 shows how the debate around the causes of balancing selection are still focussed on the allele, not the haplotype. There is other material in the quotation that is contentious: for example, the proposed timescales for the relationship between host allele frequency and the temporal development of susceptibility to pathogens. Some of the theoretical conceptualisation could, in principle, be transferred to the haplotype. However, the *intra*-locus interactions that generate positive epistasis in haplotypes largely erode a theory of independent *inter*-allelic HA, since the other allelic partners in *cis* determine the value of a particular allelic contribution to fitness. Moreover, heterozygote advantage at allelic level is unlikely to be a major driver of HLA polymorphism unless all alleles have near-identical fitnesses [74, 75, 76], a requirement that appears to be at odds with the evidence.

Rare allele advantage can also be criticized for a number of reasons. Although it is capable of generating large numbers of alleles on Takahata and Nei’s analytic theory, their turnover is rapid and their persistence times are insufficient to account for trans-species polymorphism (TSP). Where parameter values are sufficient for TSP, allele frequencies have a fairly even distribution. Again, an expectation that is not in line with the evidence, either for allele or haplotype distributions.

The principal objections to HA, NFDS, and divergent allele advantage (DAA) as explanations of HLA polymorphism are that they are purely genetic explanations and they focus on alleles. They ignore the epidemiology of infection, which has a strong density dependence for transmission, including an all-important density-dependent threshold. Combining genetics and epidemiology [32], allows one to approach HLA polymorphism from an alternative direction:

- introducing density as the source of raw data, rather than frequency, avoids the risk that frequencies will be seen implicitly as coupled.
- densities allow the introduction of rate equations based on principles of mass action (or parallels), providing access to a range of demographic models.
- host densities can be governed by disease transmission, thereby coupling capping of HLA haplotype population densities to their susceptibilities in presenting pathogen-derived peptide.
- capping of HLA haplotypes under selection automatically reduces their effective fitness to zero, creating the potential for stable capped populations at steady-state.
- the models include the combination of first-order/exponential population expansion with density-dependent mortality terms, as originally proposed by Verhulst. These can cap or regulate populations in a density-dependent manner, leading to use of logistic equations, the Lotka-Volterra competition equations, much of the mathematical theory behind the stability or otherwise of complex communities, etc.
- Lotka-Volterra competition equations provide access to a very large body of theoretical work associated with complex communities of Linnean species, through the simple expedient of treating genetic polymorphism as a problem of molecular species such as haplotypes within a single Linnean species.
- the actions of Natural Selection then emerge as distinctive HLA haplotypes that appear as capped silos through the action of density-limited growth, competitive exclusion, and limiting similarity.

On the basis of the last bullet point, balancing selection could be said to be an artefact of a focus on frequency since the density of one pathogen-limited silo need have no connection to the size of others. They would be established independently by the relationship between a haplotype and its carrier's susceptibility to disease.

However, the analysis in this paper supports the view that balancing selection is real and the direct result of selection and partitioning on haplotype fitnesses as represented by their frequencies. The 350-1850 HLA haplotypes under selection form an inter-related network by permutation of the 137 alleles that are themselves capable of demonstrating positive epistasis. A feature of the network is the orderliness of the rank distribution frequencies. There is an obvious mechanism by which this might occur: through fine tuning both of antigen-binding sites and their epistatic effects in haplotypes. The network or cloud then becomes self-regulating, and balancing selection is reinstated. One could then argue that the network is optimised to

resist pathogens, with a function of sexual reproduction being to generate the panmixis needed for network equilibration.

There is a conceptual overlap between an HLA network of this type and features of both Fisher's geometric model and a quasi-species of the type proposed by Eigen, McCaskill and Schuster (the EMS) model [77].

Fisher's geometric model has its origin in a brief mention in [69], pp. 38-41. An organism is characterised by a set of independent phenotypic traits. All phenotypes are posited as being under stabilising selection, with each having an optimal value. This creates the potential for an optimum combination of phenotypic values.

Applied to an HLA network, HLA alleles can be regarded as mutants with fitness optimisation within their respective silos. Haplotypes are independent traits that combine to produce an optimum HLA network.

The EMS model, by contrast, focuses on the molecular or genetic inter-connectedness of the components of the cloud or network, whose components differ one from another by mutation. There are no independent traits. Both Fisher's geometric model and the EMS model share a context of open-ended population expansion, disguised to some extent by use of frequencies. However, the EMS model explicitly acknowledges Fisher's fitness as a first-order rate constant, and deals with the exponential increase in density of the reactants by constant dilution and injection of fresh reagents to create a steady-state. An inherent property of the EMS is that natural selection acts rapidly to eliminate variance. Variance is maintained by high mutation rates.

Our model obviates the need for the high mutation rates of the EMS model by introducing negative density-dependent selection (NDDS) of hosts imposed by a complex, reflexive, and antagonistic environment. Obviating the need for rapid mutation allows room for a quasi-species model with much slower rates of mutation and recombination.

An important feature of quasi-species is their connectedness. Connectedness for DNA sequences is demonstrable at the nucleotide level by noting the number of differences from a reference sequence; this can be calculated as a Hamming distance. Strictly, there is no equivalent reference sequence for an HLA quasi-species, because the major haplotypes are independently stabilised into distinct silos. We can, however, infer a degree of connectedness for alleles by noting distributions, as illustrated in Fig.8. The top two panels show the distribution of allele appearances in rank order to 37,000. We have argued that the 350-1850 haplotypes of lowest rank have the rank and frequency they do because of positive selection on haplotypes with epistatic interactions between alleles and extensive pleiotropy. These haplotypes then feed all lower haplotype frequencies, mainly by recombination but also by mutation. The presence of a single allele across hundreds of separate haplotypes indicates a high degree of connectedness or pleiotropy. By contrast, the third panel shows the distribution for an allele, A*01:03g, that barely shows any epistatic contribution. It fails to be represented in any haplotype of high frequency, and populates weakly the lower frequency haplotype spectrum. The conclusion is that connectedness and pleiotropy are both low in low-frequency alleles. This is consistent with the conclusions summarised in 4.1 above.

In summary, there are three levels of positive epistatic selection acting on the HLA transplantation loci.

- at the level of the polypeptide chain. All proteins that have biological activity repre-

sent the effects of positive epistasis within their gene product, since inter-amino-acid segregation would fundamentally erode genetic transmission of successful mutants.

- at the level of the allele. Positive epistasis is manifested in some haplotypes by some combinations of the high-frequency allelic category but not others. High allelic frequencies arise by selection on haplotypes. However, such is the extent of their pleiotropy that high-frequency alleles still have frequencies that fall well short of frequencies needed to produce high-frequency haplotypes without epistasis and linkage disequilibrium.
- at the level of the haplotype. A relatively small number of alleles generate a larger catalogue haplotypes. These haplotypes form a balanced network that is optimised by shunting selection down onto alleles. Selection is further shunted to the polypeptide sequences in the ABS.

4.4 The pathogen environment

It is axiomatic that the pathogen environment exercises selection on human hosts. This generates HLA polymorphism as a signature; that is, balkanisation of host genotypes. Balkanisation of hosts takes individual genotypes below a transmission threshold, and this offers an important epidemiological protection.

HLA polymorphism must equally exert selection on pathogens. In our view, its principal effect is a reciprocal balkanisation of the pathogen environment. Balkanisation reduces the fitness gains that can be made by pathogens when they exploit genetic gaps in host defences. The number of distinct HLA genotypes under selection (350-1850) gives an approximate indication of the size of the pathogen environment that is 'seen' by the host since, superficially, a host genotype that is stably under selection requires a distinct selective agent. The pathogen landscape shows complex epidemiological behaviours [53] including development of strains. Collectively, these agencies may greatly exceed the number of haplotypes under selection. On the other hand, it may be that not all human pathogens are present simultaneously, and that strains represent a numerical amplification to fill an available niche.

Indeed, it is possible to account, in general terms, for much of pathogen behaviour as being constrained by a finite density of hosts (even if these include animals), within which the principles of competitive exclusion and limiting displacement occur. It may also be that hosts and pathogens show evidence of character displacement.

4.5 Future directions

There are a number of ways in which the ideas in this paper can be explored further. Here are obvious ones:

- HLA allelic combinations and positive epistasis. A conclusion of this paper is that the HLA haplotype distribution reflects selection on positive epistasis within certain HLA allelic combinations. The precise origin of the positive epistasis is currently unknown. It may simply reflect greater breadth of pathogen-peptide binding. However, we should note cautionary evidence, of which [78] is an example. Other explanations

include differences in stimulating T-cells. Alphafold appears capable of making major contributions [79].

- Functional overlaps of current haplotype networks. The NMDP databases include HLA frequency data on a range of self-declared ethnicities in addition to the Caucasian set. Preliminary inspection indicates that the features identified in the Caucasian set - orderly rank order distributions for alleles and haplotypes, evidence of positive epistasis, etc. - hold true for other ethnicities. It should be possible rapidly to establish their network characteristics and the extent to which the HLA datasets for other ethnicities differ functionally. It is theoretically possible that the HLA haplotype network was established only once, and has co-evolved with the pathogen environment. Features that would support long-term evolution of a single network include the stabilisation offered by the pleiotropic properties of key alleles. These potentially stabilise the trans-species polymorphism of class II alleles, and the putative survival of Neanderthal/Denisovan class I alleles.
- Frequency stability of HLA networks. A key component of the current proposal is the short-term frequency stability of the HLA haplotype network. Data from historic population movements such as that into Western Europe some 25,000 years ago may be able to clarify whether this is the case. Nearer to the present day are population shocks such as that caused by plague in Western Europe, notably the Black Death, which would have profoundly damaged the prevailing HLA network of the day. There is widespread distribution of plague pits in Western Europe that can be dated. There are, of course, technical difficulties in sequencing the HLA region, but we only really need the frequencies of the binding sites of the transplantation alleles.
- Discovery of infection matrices. Blanket pathogen sequencing, of the kind described in [80], should help define a library of pathogen peptides that could be presented. It should be possible to couple this with peptide-recognition properties of HLA haplotypes to generate infection matrices that associate particular haplotypes with particular pathogen genotypes [81].

References

- [1] K. Murphy, C. Weaver, and L. Berg. *Janeway's Immunobiology*. Norton, W.W. & Company, Inc., 10th edition, 2022.
- [2] N. Slater et al. Power laws for heavy-tailed distributions: modeling allele and haplotype diversity for the national marrow donor program. *PLoS Comput. Biol.*, 11:e1004204, 2015.
- [3] K. L. Bubb et al. Scan of human genome reveals no new loci under ancient balancing selection. *Genetics*, 173:2165–2177, 2006.
- [4] V. Soni, M. Vos, and A. Eyre-Walker. A new test suggests hundreds of amino acid polymorphisms in humans are subject to balancing selection. *PLoS Biol.*, 20:e3001645, 2022.

- [5] I. Alter, L. Gragert, S. Fingerson, M. Maiers, and Y. Louzoun. HLA class I haplotype diversity is consistent with selection for frequent existing haplotypes. *PLoS Comput. Biol.*, 13:e1005693, 2017.
- [6] A. L. Hughes and M. Yeager. Natural selection at major histocompatibility complex loci of vertebrates. *Annu. Rev. Genet.*, 32:415–435, 1998.
- [7] L. Abi-Rached et al. The shaping of modern human immune systems by multiregional admixture with archaic humans. *Science*, 334:89–94, 2011.
- [8] J. Robinson et al. Distinguishing functional polymorphism from random variation in the sequences of >10,000 HLA-A, -B and -C alleles. *PLoS Genet.*, 13:e1006862, 2017.
- [9] J. Klein. Origin of major histocompatibility complex polymorphism: the trans-species hypothesis. *Hum. immunol.*, 19:155–162, 1987.
- [10] J. Klein, A. Sato, and N. Nikolaidis. Mhc, tsp, and the origin of species: from immunogenetics to evolutionary genetics. *Annu. Rev. Genet.*, 41:281–304, 2007.
- [11] E. M. Leffler et al. Multiple instances of ancient balancing selection shared between humans and chimpanzees. *Science*, 339:1578–1582, 2013.
- [12] A. Sette and J. Sidney. Nine major HLA class I supertypes account for the vast preponderance of HLA-A and -B polymorphism. *Immunogenetics*, 50:201–212, 1999.
- [13] Y. Shen, J. M. Parks, and J. C. Smith. HLA class I supertype classification based on structural similarity. *J. Immunol.*, 210:103–114, 2023.
- [14] R. Dawkins et al. Genomics of the major histocompatibility complex: haplotypes, duplication, retroviruses and disease. *Immunol. Rev.*, 167:275–304, 1999.
- [15] A. Albrechtsen, I. Moltke, and R. Nielsen. Natural selection and the distribution of identity-by-descent in the human genome. *Genetics*, 186:295–308, 2010.
- [16] B. S. Penman, B. Ashby, C. O. Buckee, and S. Gupta. Pathogen selection drives nonoverlapping associations between HLA loci. *Proc. Natl. Acad. Sci. U. S. A.*, 110:19645–19650, 2013.
- [17] R. Nielsen. Molecular signatures of natural selection. *Annu. Rev. Genet.*, 39:197–218, 2005.
- [18] D. Meyer, V. R. C. Aguiar, B. D. Bitarello, D. Y. C. Brandt, and K. Nunes. A genomic perspective on HLA evolution. *Immunogenetics*, 70:5–27, 2018.
- [19] R. M. Anderson and R. M. May. Population biology of infectious diseases: Part I. *Nature*, 280:361–367, 1979.
- [20] L. J. Buckingham and B. Ashby. Coevolutionary theory of hosts and parasites. *J. Evol. Biol.*, 35:205–224, 2022.

- [21] P. Chesson and J. J. Kuang. The interaction between predation and competition. *Nature*, 456:235–238, 2008.
- [22] P. Chesson. Updates on mechanisms of maintenance of species diversity. *J. Ecol.*, 106: 1773–1794, 2018.
- [23] P.-F. Verhulst. Notice sur la loi que la population suit dans son accroissement. *Correspondance Mathématique et Physique.*, 10:113–121, 1838.
- [24] P.-F. Verhulst. Recherches mathématiques sur la loi d’accroissement de la population. *Nouveaux mémoires de l’Académie Royale des Sciences et Belles-Lettres de Bruxelles*, 18:1–38, 1845.
- [25] R. A. Neher and B. I. Shraiman. Competition between recombination and epistasis can cause a transition from allele to genotype selection. *Proc. Natl. Acad. Sci. U. S. A.*, 106: 6866–6871, 2009.
- [26] R. M. May. Parasitic infections as regulators of animal populations. *Am. Sci.*, 71:36–45, 1983.
- [27] W. O. Kermack and A. G. McKendrick. A contribution to the mathematical theory of epidemics. *Proc. R. Soc. Lond. A*, 115:700–721, 1927.
- [28] W. O. Kermack and A. G. McKendrick. Contributions to the mathematical theory of epidemics. ii. the problem of endemicity. *Proc. R. Soc. Lond. A*, 138:55–83, 1932.
- [29] W. O. Kermack and A. G. McKendrick. Contributions to the mathematical theory of epidemics. iii. further studies of the problem of endemicity. *Proc. R. Soc. Lond. A*, 141: 94–122, 1933.
- [30] R. M. Anderson. The regulation of host population growth by parasitic species. *Parasitology*, 76:119–157, 1978.
- [31] R. M. Anderson. Discussion: The kermack-mckendrick epidemic threshold theorem. *Bull. Math. Biol.*, 53:3–32, 1991.
- [32] R. M. May and R. M. Anderson. Epidemiology and genetics in the coevolution of parasites and hosts. *Proc. R. Soc. Lond. B, Biol. Sci.*, 219:281–313, 1983.
- [33] R. M. May. *Stability and complexity in model ecosystems*. Princeton University Press, princeton landmarks in biology edition, 2001.
- [34] L. Euler. *Introductio in analysin infinitorum*. Bosquet: Lucerne, 1748.
- [35] L. Euler. Recherches générales sur la mortalité et la multiplication du genre humain. *Mémoires de l’Académie des Sciences de Berlin*, 16:144–164, 1767.
- [36] D. Klyve. Darwin, malthus, süssmilch, and euler: the ultimate origin of the motivation for the theory of natural selection. *J. Hist. Biol.*, 47:189–212, 2014.

- [37] T. R. Malthus. *An Essay on the Principle of Population, etc.* J. Johnson, 1798.
- [38] A. G. M'Kendrick and M. Kesava Pai. The rate of multiplication of micro-organisms: a mathematical study. *Proc. R. Soc. Edin.*, 31:649–653, 1912.
- [39] R. Pearl and L. J. Reed. On the rate of growth of the population of the united states since 1790 and its mathematical representation. *Proc. Natl. Acad. Sci. U. S. A.*, 6:275–288, 1920.
- [40] J. Mallet. The struggle for existence: How the notion of carrying capacity, k , obscures the links between demography, darwinian evolution, and speciation. *Evol. Ecol. Res.*, 14:627–665, 2012.
- [41] S. A. Levin. Community equilibria and stability, and an extension of the competitive exclusion principle. *Am. Nat.*, 104:413–423, 1970.
- [42] R. H. MacArthur. Patterns of communities in the tropics. *Biol. J. Linn. Soc. Lond.*, 1: 19–30, 1969.
- [43] R. MacArthur. Species packing and competitive equilibrium for many species. *Theor. Popul. Biol.*, 1:1–11, 1970.
- [44] J. E. Cohen and C. M. Newman. A stochastic theory of community food webs i. models and aggregated data. *Proc. R. Soc. Lond. B*, 224:421–428, 1985.
- [45] R. Law and U. Dieckmann. A dynamical system for neighbourhoods in plant communities. *Ecology*, 81:2137–2148, 2000.
- [46] J. Bascompte and P. Jordano. Plant-animal mutualistic networks: the architecture of biodiversity. *Annu. Rev. Ecol. Evol. Syst.*, 38:567–593, 2007.
- [47] R.A. Neher, M. Vucelja, M. Mezard, and B.I. Shraiman. Emergence of clones in sexual populations. *J. Stat. Mech.: Theory Exp.*, page P01008, 2013.
- [48] V. Belevitch. On the statistical laws of linguistic distributions. *Ann. Soc. Sci. Brux.*, 73: 301–326, 1959.
- [49] R. M. Gardner and W. R. Ashby. Connectance of large (dynamic) systems: critical values for stability. *Nature*, 228:784, 1970.
- [50] R. M. May. Will a large complex system be stable? *Nature*, 238:413–414, 1972.
- [51] Y. Krumbeck, Q. Yang, G. W. A. Constable, and T. Rogers. Fluctuation spectra of large random dynamical systems reveal hidden structure in ecological networks. *Nat. Commun.*, 12:3625, 2021.
- [52] Microbiology by numbers. *Nat. Rev. Microbiol.*, 9:628, 2011.
- [53] S. Gupta. Darwin review: the evolution of virulence in human pathogens. *Proc. R. Soc. Lond. B*, 291:20232043, 2024.

- [54] D. J. Barker et al. The ipd-imgt/hla database. *Nucleic Acids Res.*, 51(D1):D1053–D1060, 2023.
- [55] L. Gragert, A. Madbouly, J. Freeman, and M. Maiers. Six-locus high resolution hla haplotype frequencies derived from mixed-resolution dna typing for the entire us donor registry. *Hum. Immunol.*, 74:1313–1320, 2013.
- [56] R. Margalef. *Perspectives in Ecological Theory*. University of Chicago, 1968.
- [57] J. Zhang. Patterns and evolutionary consequences of pleiotropy. *Annu. Rev. Ecol. Evol. Syst.*, 54:1–19, 2023.
- [58] W. Klitz, P. Hedrick, and E. J. Louis. New reservoirs of hla alleles: pools of rare variants enhance immune defense. *Trends Genet.*, 28:480–486, 2012.
- [59] J. Sidney, B. Peters, N. Frahm, C. Brander, and A. Sette. HLA class I supertypes: a revised and updated classification. *BMC Immunol.*, 9:1, 2008.
- [60] K. E. Langergraber et al. Generation times in wild chimpanzees and gorillas suggest earlier divergence times in great ape and human evolution. *Proc. Natl. Acad. Sci. U. S. A.*, 109:15716–15721, 2012.
- [61] N. G. de Groot et al. Evidence for an ancient selective sweep in the mhc class i gene repertoire of chimpanzees. *Proc. Natl. Acad. Sci. U. S. A.*, 99:11748–11753, 2002.
- [62] J. W. Gregersen et al. Functional epistasis on a common mhc haplotype associated with multiple sclerosis. *Nature*, 443:574–577, 2006.
- [63] M. Carrington. Recombination within the human mhc. *Immunol. Rev.*, 167:245–256, 1999.
- [64] Ahmad et al. Haplotype-specific linkage disequilibrium patterns define the genetic topography of the human mhc. *Hum. Mol. Genet.*, 12:647–656, 2003.
- [65] J. B. S. Haldane. Disease and evolution. *Ric. Sci. Supplement*, 19:68–76, 1949.
- [66] P. W. Hedrick and W. Klitz. Evolution of the human mhc: New haplotype frequency analysis is not informative. *Proc. Natl. Acad. Sci. U. S. A.*, 116:23386–23387, 2019.
- [67] H J Muller. Genetic variability, twin hybrids and constant hybrids, in a case of balanced lethal factors. *Genetics*, 3:422–499, 1918.
- [68] E B Ford. Polymorphism. *Biological Reviews*, 20:73–88, 1945.
- [69] R. A. Fisher. *The Genetical Theory of Natural Selection - A Complete Variorum Edition*. Oxford University Press, Oxford, 1999.
- [70] I. J. Saccheri, F. Rousset, P. C. Watts, P. M. Brakefield, and L. M. Cook. Selection and gene flow on a diminishing cline of melanic peppered moths. *Proc. Natl. Acad. Sci. U. S. A.*, 105:16212–16217, 2008.

- [71] M. Slatkin. Joint estimation of selection intensity and mutation rate under balancing selection with applications to hla. *Genetics*, 221:iyac058, 2022.
- [72] N. Takahata and M. Nei. Allelic genealogy under overdominant and frequency-dependent selection and polymorphism of major histocompatibility complex loci. *Genetics*, 124:967–978, 1990.
- [73] L. G. Spurgin and D. S. Richardson. How pathogens drive genetic diversity: Mhc, mechanisms and misunderstandings. *Proc. Biol. Sci.*, 277:979–988, 2010.
- [74] R. C. Lewontin, L. R. Ginzburg, and S. D. Tuljapurkar. Heterosis as an explanation for large amounts of genic polymorphism. *Genetics*, 88:149–169, 1978.
- [75] R. J. De Boer, J. A. Borghans, M. van Boven, C. Keşmir, and F. J. Weissing. Heterozygote advantage fails to explain the high degree of polymorphism of the mhc. *Immunogenetics*, 55:725–731, 2004.
- [76] T. Stefan et al. Divergent allele advantage provides a quantitative model for maintaining alleles with a wide range of intrinsic merits. *Genetics*, 212:553–564, 2019.
- [77] M. Eigen, J. McCaskill, and P. Schuster. Molecular quasi-species. *J. Phys. Chem.*, 92:6881–6891, 1988.
- [78] X. Rao, R. J. De Boer, D. van Baarle, M. Maiers, and C. Kesmir. Complementarity of binding motifs is a general property of hla-a and hla-b molecules and does not seem to effect hla haplotype composition. *Front. Immunol.*, 4:374, 2013.
- [79] B. McMaster, C. Thorpe, G. Ogg, C. M. Deane, and H. Koohy. Can alphafold’s breakthrough in protein structure help decode the fundamental principles of adaptive cellular immunity? *Nat. Methods*, 21:766–776, 2024.
- [80] O. Özer and T. L. Lenz. Unique pathogen peptidomes facilitate pathogen-specific selection and specialization of mhc alleles. *Mol. Biol. Evol.*, 38:4376–4387, 2021.
- [81] H. Märkle et al. Inference of host–pathogen interaction matrices from genome-wide polymorphism data. *Mol. Biol. Evol.*, 41:msae176, 2024.